



University of Cologne

**Distribution of zooplankton in relation to an
upwelling filament off Namibia**

Bachelor Thesis

Sarah Fitzek

1st Supervisor: Prof. Dr. E. von Elert

2nd Supervisor: Prof. Dr. C. Möllmann



University of Hamburg

Institute for Hydrobiology and Fisheries Science

Abstract

The Benguela Current region in Namibia is one of the four biggest coastal upwelling systems in the world. The cold upwelling nutrient rich water causes an exceptionally high primary production, which results in increasing stocks of zooplankton and higher trophic levels (e.g. fish, Coelenterata). The population in the upper water layer can be exported offshore by advection in the open ocean within upwelling filaments.

In October 2010 an offshore upwelling filament in the Benguela Current was detected and the zooplankton was successfully sampled with a multiple closing net of 333 μm mesh aperture on board of the British RRS Discovery. The aim of the present study was part of the GENUS project (Geochemistry and Ecology of the Namibian Upwelling System), which clarifies the relationship between the biogeochemical cycles and the ecosystem structure in this region. The samples have been analysed to compare the abundance and composition of the mesozooplankton inside and outside of the filament water. Surprisingly, significantly higher zooplankton biomasses and abundances were detected in the water mass, which was identified as outside of the filament by hydrographic parameters. In detail, Crustacea and Copepoda generally showed significantly higher abundances outside of the filament. However, inside of the filament, higher relative abundances of Copepoda Calanoida, Euphausiacea, Malacostraca, Crustacea larvae, Amphipoda, and Chaetognatha were detected. This distribution pattern coincides with lower chl-*a* fluorescence within the upwelling water compared to outside of the filament. Possible causes like mortality, opposite direction currents, top-down controlling, or general instabilities of the upwelling structures are discussed.

Table of Contents

Abstract.....	I
Table of Contents.....	II
List of Tables	III
List of Figures	VI
1. Introduction	1
1.1. Upwelling systems	1
2. Materials and methods	6
2.1. Sampling.....	6
2.2. Sample analyses	10
3. Results.....	13
3.1. Hydrography	13
3.2. Distribution of Biomass	15
3.3. Distribution of zooplankton.....	18
4. Discussion	25
4.1. Hydrographical characterisation	25
4.2. Biological characterisation	26
4.3. Critical evaluation of methods.....	32
4.4. Outlook	33
References	34
Acknowledgements - Danksagungen.....	41
Appendix.....	42
Eidesstattliche Erklärung	51

List of Tables

1. Sampling details of the MOCNESS haul in the upwelling filament in the northern Benguela Current system in October 2010. Local time = UTC (Universal Time Coordinated) + 2h.
2. Sampling data of the MOCNESS haul on October 3rd 2010. * = taxonomically analysed. L = Left nets, R = Right nets. Values for sampling depths, temperature, and salinity are means of detailed records.
3. Zooplankton aliquots of different size fractions for all nets, which were determined by counting.
4. Mesozooplankton taxa in the detected filament in the northern Benguela Current system.
5. Biomass concentrations expressed as wet weight ($\text{mg} \cdot 1000 \text{ m}^{-3}$) in subsurface water (SSW: L2), water mass 'A' (WMA: L4, L5, L7), transition water (TW: L8, R2, R3), and water mass 'B' (WMB: R4, R6, R8). P-values of simultaneous t-test for the single fractions after an adjustment according to *Bonferroni*
6. Abundances of the zooplankton expressed as individuals * 1000 m^{-3} (sum of size fractions $\leq 5 \text{ mm}$) in water mass 'A' (WMA: L4, L5, L7) and water mass 'B' (WMB: R4, R6, R8). P-values simultaneous of t-test for the single fractions after an adjustment according to *Bonferroni*.

7. Numerical and relative abundances in the MOCNESS nets (sum of size fractions ≤ 5 mm) in water mass 'A' (WMA: L4, L5, L7) and water mass 'B' (WMB: R4, R6, R8). P-values of simultaneous t-tests for the abundances were adjusted according to *Bonferroni*. (N / A) p-values could not be determined due to zero values.

 8. Dominance (+) of taxa with relative abundance > 1 % in water mass 'A' (WMA: L4, L5, L7) or water mass 'B' (WMB: R4, R6, R8).
-
- A.1. Biomass of zooplankton in the MOCNESS nets in all sieve fractions expressed as wet weight ($\text{mg} * 1000 \text{ m}^{-3}$).

 - A.2. Abundances of zooplankton in the MOCNESS nets in all sieve fractions expressed as individuals $* 1000 \text{ m}^{-3}$.

 - A.3. Total abundances of mesozooplankton in net L4 of the MOCNESS haul on October 3rd 2010 in all sieve fractions, expressed as individuals $* 1000 \text{ m}^{-3}$.

 - A.4. Total abundances of mesozooplankton in net L5 of the MOCNESS haul on October 3rd 2010 in all sieve fractions, expressed as individuals $* 1000 \text{ m}^{-3}$.

 - A.5. Total abundances of mesozooplankton in net L7 of the MOCNESS haul on October 3rd 2010 in all sieve fractions, expressed as individuals $* 1000 \text{ m}^{-3}$.

 - A.6. Total abundances of mesozooplankton in net L8 of the MOCNESS haul on October 3rd 2010 in all sieve fractions, expressed as individuals $* 1000 \text{ m}^{-3}$.

A.7. Total abundances of mesozooplankton in net R4 of the MOCNESS haul on October 3rd 2010 in all sieve fractions, expressed as individuals * 1000 m⁻³.

A.8. Total abundances of mesozooplankton in net R6 of the MOCNESS haul on October 3rd 2010 in all sieve fractions, expressed as individuals * 1000 m⁻³.

A.9. Total abundances of mesozooplankton in net R8 of the MOCNESS haul on October 3rd 2010 in all sieve fractions, expressed as individuals * 1000 m⁻³.

List of Figures

1. Ocean surface currents (black arrows) driven by the major wind fields (blue arrows); after Lumpkin, unpublished results.
2. Schematic view on Ekman transport. Arrows show wind-driven surface water transport (at an angle of 45°) and induced orthogonal Ekman transport.
3. Schematic view on origin of coastal upwelling. Arrows indicate surface water flow in offshore direction and replacement by upwelling deep water.
4. Upwelling activity on October 3rd 2010 in the northern Benguela Current region recorded by satellite image of sea surface temperature (SST, $^\circ\text{C}$). Sampling location shows the stations of zooplankton sampling between 18.67°S and 18.85°S at 10.65°E on the southern border of the upwelling filament; after Muller, unpublished results.
5. Distribution of temperature ($^\circ\text{C}$) in the upper 100 m of the upwelling filament in the Benguela Current region in October 2010 at 11°E ; after Muller, unpublished results.
6. Sampling location between 18.67°S and 18.85°S on a longitudinal transect at 10.65°E in the northern Benguela Upwelling region off Namibia; after Ocean Data View, unpublished results. The cruise 356 of RRS Discovery started at Walvis Bay.
7. Schematic view on a MOCNESS haul.

8. Picture of a 1 m²-Double-MOCNESS device with 18 nets (9 left nets, 9 right nets) with a mesh size of 333 μm .
9. Sampling strategy of MOCNESS haul in $\sim 35 - 50$ m water depth.
L1 - L9 = Left nets, R1 - R9 = right nets.
10. Horizontal profile of water temperature ($^{\circ}\text{C}$) and salinity (PSU) in the Benguela Upwelling system on October 3rd 2010 at latitudes from 18.67 $^{\circ}\text{S}$ to 18.85 $^{\circ}\text{S}$ along the longitudinal transect at 10.65 $^{\circ}\text{E}$ for ~ 22 km.
11. Profile of water temperature ($^{\circ}\text{C}$) and salinity (PSU) of the MOCNESS haul in subsurface water (SSW), water mass 'A' (WMA), transition water (TW), and water mass 'B' (WMB).
12. Biomass concentrations for the MOCNESS nets (sum of size fractions ≤ 5 mm) in subsurface water (SSW), water mass 'A' (WMA), transition water (TW), and water mass 'B' (WMB).
13. Composition of zooplankton biomass in the different size fractions in subsurface water (SSW: L2), water mass 'A' (WMA: L4, L5, L7), transition water (TW: L8, R2, R3), and water mass 'B' (WMB: R4, R6, R8).
14. Abundances of the zooplankton in the MOCNESS nets (sum of size fractions ≤ 5 mm) in subsurface water (SSW), water mass 'A' (WMA), transition water (TW), and water mass 'B' (WMB).
15. Composition of zooplankton abundance for the different size fractions in water mass 'A' (WMA: L4, L5, L7) and water mass 'B' (WMB: R4, R6, R8).

16. Abundances of Copepoda in the MOCNESS nets (sum of size fractions ≤ 5 mm) in water mass 'A' (WMA: L4, L5, L7), transition water (TW: L8, R2, R3), and water mass 'B' (WMB: R4, R6, R8).
17. Composition of (A) Chaetognatha and (B) Euphausiacea abundances of the different size fractions in water mass 'A' (WMA: L4, L5, L7) and water mass 'B' (WMB: R4, R6, R8).
18. Biomass of Copepoda, when upwelling filament was (A) present at 42.7 °N and (B) absent 41.9 °N off Oregon in USA in August 2002. Concentrations are labelled with their longitudes. Grey highlighting indicate stations within cold filaments, vertical dashed lines show the location of the upwelling front; after Keister et al. (2008).
19. (A) Upwelling activity recorded by sea surface temperature (°C) and (B) spatial abundance of Copepoda ($\text{ind. m}^{-2} * 10^{-3}$) at Mejillones Peninsula in Chile (23.3 °S, 70.6 °W) in December 1996. Filled circles represent locations, that were grouped as belonging to upwelling-type conditions, open squares are non-upwelling type locations determined water temperature; after Escribano & Hidalgo (2000).
20. The model system of Lotka-Volterra with periodic populations of prey (red line) and predators (blue line).
21. Chlorophyll-*a* concentration related to upwelling activity off (A) Portugal; after Cravo et al. (2010) and (B) Chile; after Escribano & Hidalgo (2000).

1. Introduction

1.1. Upwelling systems

The global wind fields induce ocean surface currents. At the edges of the ocean they turn into western and eastern boundary currents (Fig. 1). Western boundary currents (e.g. Gulf Stream in the Atlantic Ocean, Kuroshio in the Pacific Ocean) transport warm water polewards, whereas eastern boundary currents (e.g. Benguela Current in the Atlantic Ocean, Humboldt Current in the Pacific Ocean) conduct cold upwelling water, which flows equatorwards.

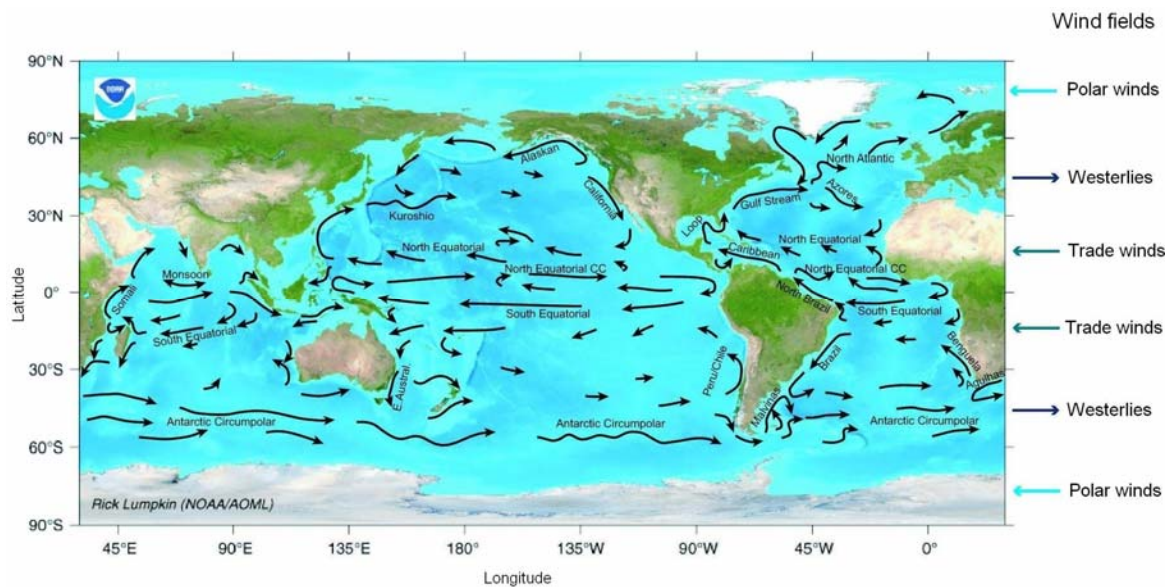


Figure 1: Ocean surface currents (black arrows) driven by the major wind fields (blue arrows); after Lumpkin, unpublished results.

The rotation of the earth creates the Coriolis force, which deflects the movement of the water on the northern hemisphere to the right and on the southern hemisphere to the left. In coastal boundary currents this results in an Ekman transport. The ocean water, divided into vertical layers, is deflected at an angle of 45 ° to the wind field or the water layers above. All Ekman layers integrated, result in a net water transport at an angle of 90 ° to the wind field (Fig. 2).

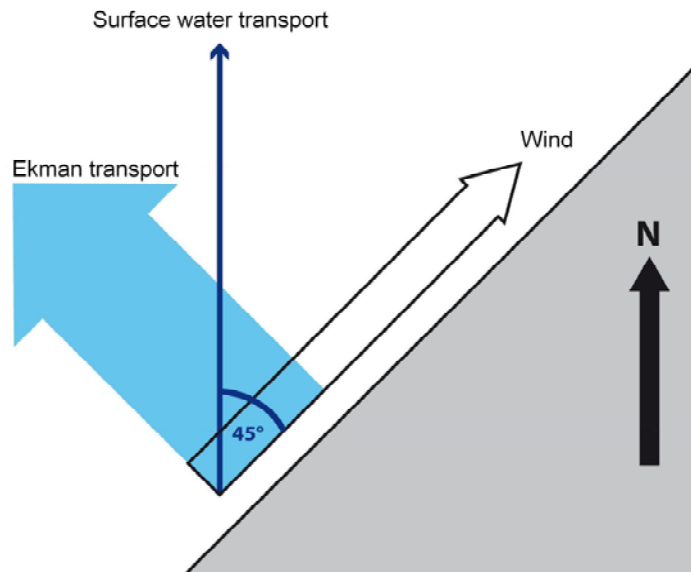


Figure 2: Schematic view on Ekman transport. Arrows show wind-driven surface water transport (at an angle of 45°) and induced orthogonal Ekman transport.

Significant vertical movement of the water may build upwelling systems, like in the Benguela region off Namibia. Upwelling occurs when the surface water is transported offshore and then replaced by cold nutrient rich deep water (Fig. 3). The nutrients induce a high primary production with large phytoplankton cells, which are then eaten by large zooplankton (mainly Copepoda). The exceptionally high primary productivity in the Benguela Current system effects increasing zooplankton abundance via the food chain (Huggett et al. 2009). The produced organic material is either recycled in the water column or sinks to the bottom (Brune et al. 1995). In upwelling systems the occurrence of additional oceanographic features like filaments is common, where the material is rapidly advected offshore (Wroblewski 1980). These upwelling filaments transport the produced zooplankton up to 100 - 500 km in offshore direction (Smith & Buseck 1982).

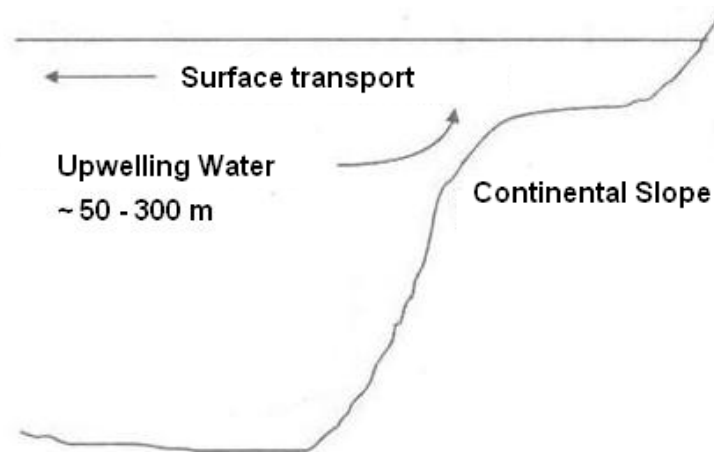


Figure 3: Schematic view on origin of coastal upwelling. Arrows indicate surface water flow in offshore direction and replacement by upwelling deep water.

The Benguela Current is one of the four biggest upwelling systems on earth and reaches an average width of 150 - 200 km. In response to the process of upwelling, the physical and biological characteristics are spatially and temporally variable and build an unstable environment (Sakko 1998). During the last decades, a change from a dominance of fish to gelatinous organisms (e.g. Coelenterata) occurred in the Benguela region (Cury & Shannon 2004), probably caused by overfishing and / or climate change. Since Coelenterata are carnivores and thus feed on the same resources as fish, overfishing will be of advantage for these gelatinous organisms.

The world's upwelling systems comprise 90 % of the global fish stocks and support major fisheries (Bianchi et al. 1999). Fish, as a source of income in, contributes to 7 % of gross national product in Namibia (MFMR 1996). The GENUS project (Geochemistry and Ecology of the Namibian Upwelling System), funded by the German Ministry of Research and Education, aims to clarify the relationship between the biogeochemical cycles and the ecosystem structure in the Benguela Current region. Strong coastal upwelling activity in the northern Benguela Current system between 18.0 and 19.3 °S at 12.5 °E in October 2010 was recorded by satellite imagery of sea surface temperature (SST, Fig. 4). Also typical filament structures occurred, in which the cold upwelling water drifted offshore up to 9 °E (see sampling location).

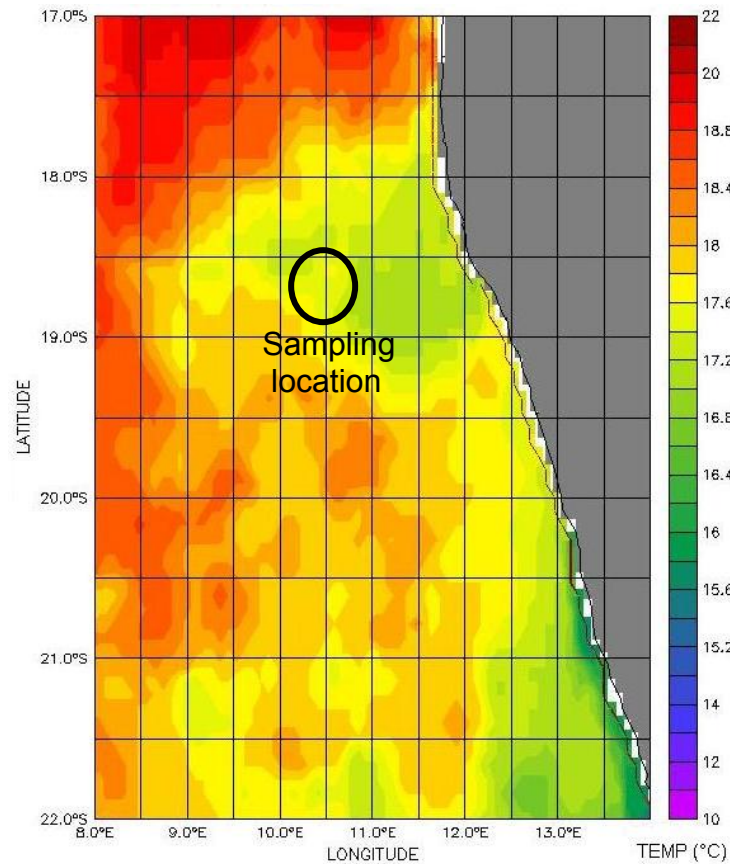


Figure 4: Upwelling activity on October 3rd 2010 in the northern Benguela Current region recorded by satellite image of sea surface temperature (SST, °C). Sampling location shows the stations of zooplankton sampling between 18.67 °S and 18.85 °S at 10.65 °E on the southern border of the upwelling filament; after Muller, unpublished results.

According to this result, zooplankton sampling in the area of an upwelling filament was inaugurated. A few days later, when the research ship arrived at the sampling station, the visibility of the filament by satellite imagery was hampered by warm surface water. However, with the use of a SCANFISH, an undulating measuring device, which was towed behind the ship, the extension of the detected upwelling filament could be measured (Fig. 5) and the zooplankton was successfully sampled on the southern border of the upwelling filament between 18.67 °S and 18.85 °S at 10.65 °E.

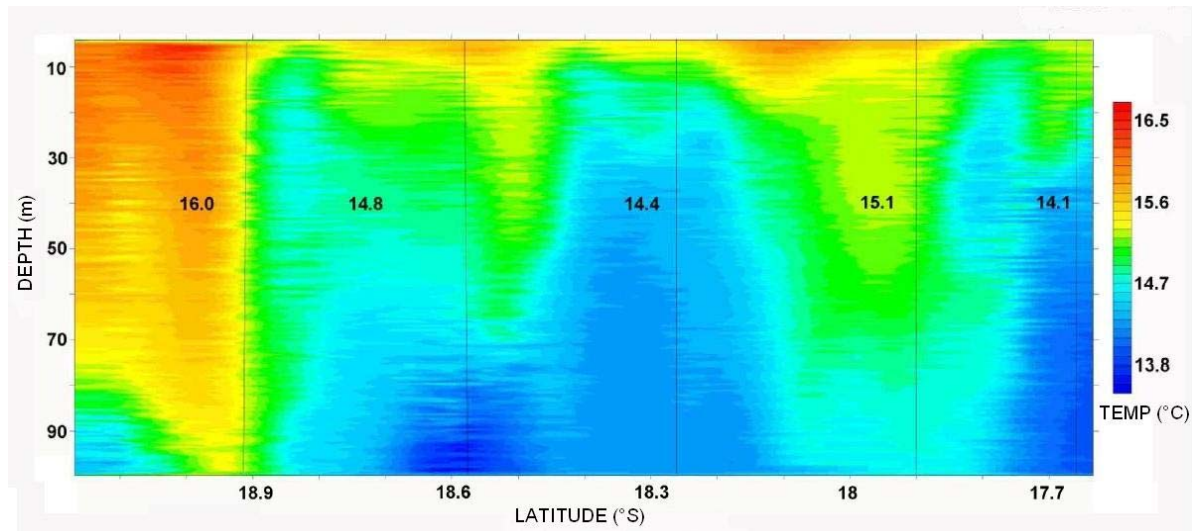


Figure 5: Distribution of temperature (°C) in the upper 100 m of the upwelling filament in the Benguela Current region in October 2010 at 11 °E; after Muller, unpublished results.

In this thesis, the correlation between the zooplankton composition inside and outside of a filament in the Benguela Current system will be compared, to test the hypothesis, that the produced zooplankton are advected for hundreds of kilometres in offshore direction via upwelling filaments. Therefore it has to be verified that the zooplankton biomass and abundance enhanced inside the filament compared to the offshore water, which is due to the exceptional conditions of filament features in the coastal upwelling region.

2. Materials and methods

2.1. Sampling

The cruise 356 of the British RRS (Royal Research Ship) Discovery started in October 2010 from Walvis Bay in Namibia for the project GENUS (Geochemistry and Ecology of the Namibian Upwelling System). During the track, an upwelling filament in the northern Benguela region was detected and intensively investigated by physical oceanographers. On October 3rd 2010 the filament was sampled on a longitudinal transect at 10.65 °E between 18.67 °S and 18.85 °S (Fig. 6, Tab. 1). Sampling started at 17:11 UTC (Universal Time Coordinated) at night, i.e. 19:11 local time, with a ship's speed of 2 knots (ca. 1 m / s). The sampling stations were located at the southern border of the upwelling filament. Sampling was performed by horizontal hauling in 30 - 50 m depth with a 1 m² Double-MOCNESS (Multiple Opening and Closing Net and Environmental sensing System; Wiebe et al. 1985). The total water depth at the MOCNESS-station was 3102 m.

Table 1: Sampling details of the MOCNESS haul in the upwelling filament in the northern Benguela Current system in October 2010. Local time = UTC (Universal Time Coordinated) + 2h.

Haul	Station	Date	Time (UTC)	Water depth (m)	Coordinates
22	35	3.10. 2010	Start:17:11 End: 23:31	3102	Start: 18.67 °S 10.65 °E End: 18.85 °S 10.65 °E

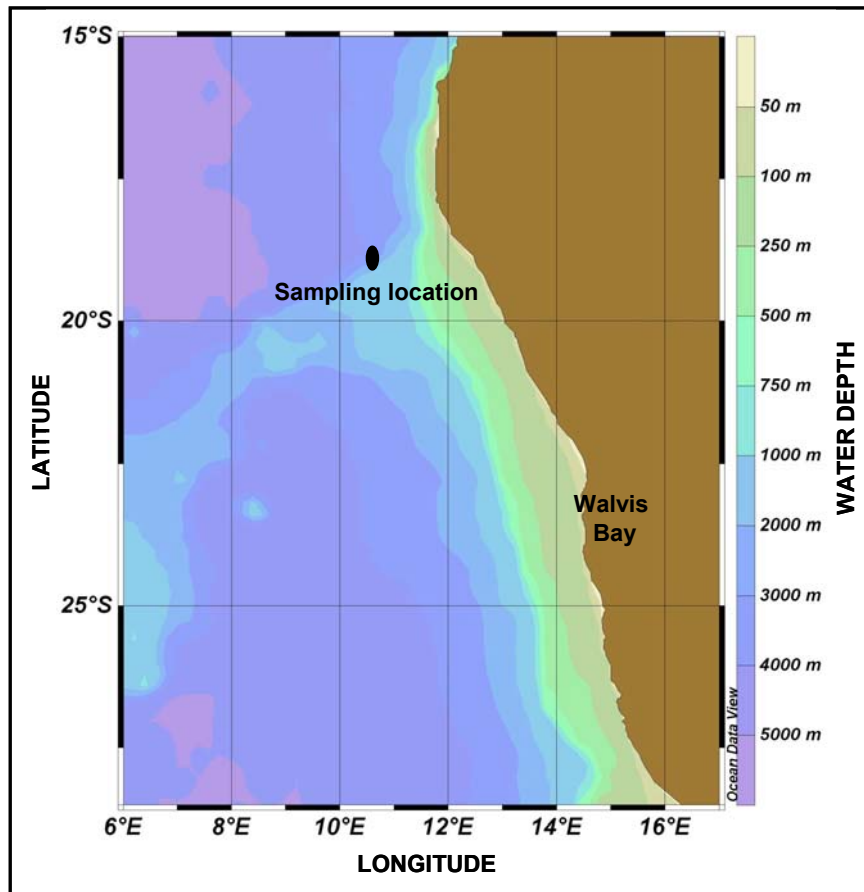


Figure 6: Sampling location between 18.67 °S and 18.85 °S on a longitudinal transect at 10.65 °E in the northern Benguela Upwelling region off Namibia; after Ocean Data View, unpublished results. The cruise 356 of RRS Discovery started at Walvis Bay.

The Double-MOCNESS consists of 18 nets (9 left nets, 9 right nets) with a mesh size of 333 μm and a mouth opening of 1 m^2 (Fig. 7 and 8). All nets can be opened and closed sequentially to allow a fine-spaced sample resolution. The filtered volume is measured by a flow meter. The device carries CTD-probes (Conductivity, Temperature, and Depth) to assess abiotic parameters. The sampling data and filtered volumes of each net are presented in Table 2, whereas the values for sampling depths, temperature, and salinity are means of continuous measurements (every 4 seconds).

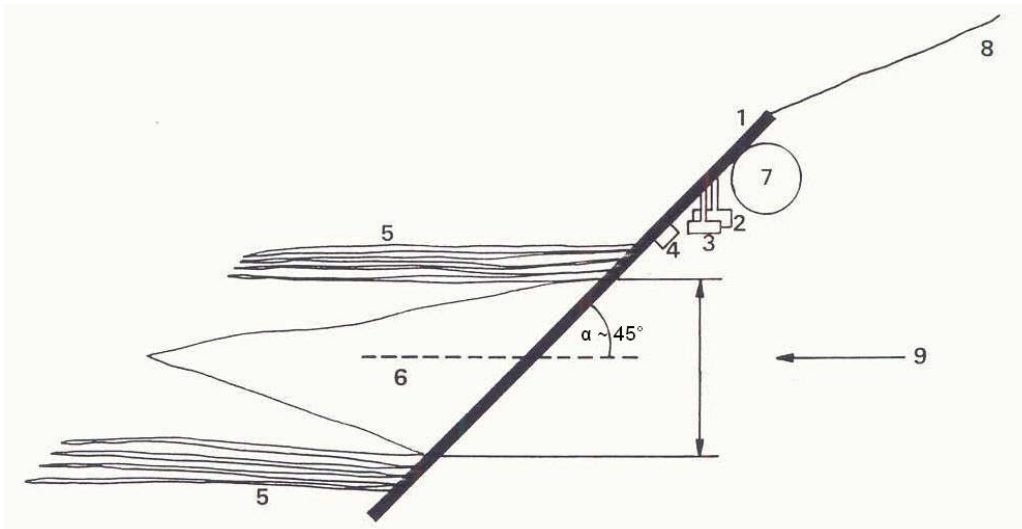


Figure 7: Schematic view on a MOCNESS haul. 1 - Frame, 2 - Temperature and salinity sensor, 3 - Flow meter, 4 - Net release motor, 5 - Closed nets, 6 - Open net, 7 - Underwater electronic device, 8 - Tow cable, 9 - Water inflow; after Koppelman (1990).



Figure 8: Picture of a 1 m²-Double-MOCNESS device with 18 nets (9 left nets, 9 right nets) with a mesh size of 333 µm.

The zooplankton sampling for this thesis was initiated with the descending nets L1 and R1, followed by the left nets L2 - L9 (Fig. 9). Then the right nets R2 - R9 were opened consecutively. Net R9 and net L9 were closed simultaneously upon ascending of the MOCNESS device on the surface.

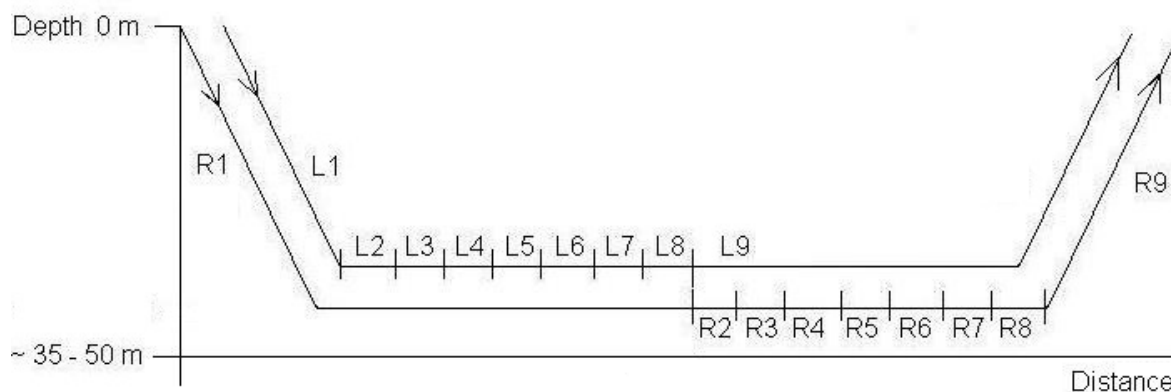


Figure 9: Sampling strategy of MOCNESS haul in ~ 35 - 50 m water depth. L1 - L9 = Left nets, R1 - R9 = right nets.

Upon recovery of the MOCNESS, the nets were rinsed with seawater. The sampled plankton was preserved immediately in a 4 % formaldehyde-seawater solution buffered with sodium-tetraborate for biomass and taxonomic analyses (Steedman 1976). Only the nets L2 and R8 were aliquoted directly after sampling, using a Motoda plankton splitter (Motoda 1959) to allow physiological measurements of some animals, which will be presented elsewhere. The descending (L1, R1) and ascending nets (L9, R9) were not included in the evaluation. Net L6 failed due to a preservation mistake. L3 and L7 have been sent to the University of Bremen for more detailed studies on fish larvae. In total, 11 samples were available for the analysis in this thesis.

2.2. Sample analyses

In the laboratory, the preserved zooplankton samples for biomass determination and taxonomic analyses were sieved into size fractions of < 0.5, 0.5 - 1, 1 - 2, 2 - 5, and > 5 mm. After placing the sieve fractions in 70 % ethanol for 30 s and drying them on tissue paper, the material was wet weighed on an analytical balance (Tranter 1962).

After weighing, the samples were transferred into a sorting fluid composed of 0.5 % propylene-phenoxetol, 5.0 % propylene-glycol, and 94.5 % fresh water (Steedman 1976). The following seven nets were chosen for sorting and counting of the mesozooplankton: L4, L5, L7, L8, R4, R6 and R8. In total 35 size-fractionated samples were taxonomically analysed. Rich zooplankton samples were aliquot with a 10 times Splitter (Wiborg 1951) according to Kott (1953) to minimize the time for counting (Tab. 3).

Table 3: Zooplankton aliquots of different size fractions for all nets, which were determined by counting.

Net #	Sieve fraction (mm)				
	< 0.5	0.5 - 1	1 - 2	2 - 5	> 5
L4	1/5	1/20	1/20	1/20	1/8
L5	1/4	1/10	1/10	1/5	1/4
L7	1/10	1/20	3/100	1/100	1/4
L8	1/50	1/50	1/50	1/20	1/10
R4	1/50	1/50	1/100	3/100	1/5
R6	1/20	1/20	1/20	1/10	1/10
R8	1/20	1/20	1/20	1/40	1/4

For the identification of functional and taxonomical groups of the mesozooplankton, the key of Gibbons (1999) about zooplankton taxonomy in the Benguela Current region was used (Tab. 4). Exuviae and carcasses, according to Wheeler (1967) and Weikert (1977), were excluded from the total counts. Furthermore, Siphonophora are not included in the counts of the total community. They are expressed as parts per volume, since they are supposed to belong to the size > 5 mm and tend to break into pieces in the nets. Total mesozooplankton is the sum of size fractions ≤ 5 mm (see also Weikert & Trinkaus 1990). Generally, animals > 5 mm are not sampled quantitatively with 333 μ m nets and were treated separately.

Table 4: Mesozooplankton taxa in the detected filament in the northern Benguela Current system.

Crustacea	Gelatinous	Fish	Undefined
Copepoda - Calanoid Copepoda - Cyclopid Copepoda	Gelatinous Organisms - Cnidaria - Ctenophora - Undefined Gelatinous	Fish larvae	Other larvae
Malacostraca & Crustacea larvae - Euphausiacea - Decapoda, Mysidacea & Crustacea larvae - Amphipoda	Semi-Gelatinous Organisms - Mollusca - Chaetognatha - Polychaeta	Fish eggs	Unknown Organisms
Ostracoda			

The biomass and numerical abundance was standardized to a volume of 1000 m³ using the following formulas:

$$\text{biomass (mg * 1000 m}^{-3}\text{)} = (\text{mg wet weight * 1000 / filtered vol.}) * \text{aliquot factor,}$$

$$\text{abundance (ind. * 1000 m}^{-3}\text{)} = (\text{individuals * 1000 / filtered vol.}) * \text{aliquot factor.}$$

A Kolmogorov-Smirnov test was performed to proof, whether the biomass and abundances represent a normal distribution. The normality test detected a probability of 99 % for the biomass and abundances, that the data are not normally distributed. To assume an approximate normal distribution it was decided to log-transform all data:

$$\text{biomass:} \quad \log(\text{mg}) = \log((\text{mg * 1000 m}^{-3}\text{)}+1),$$

$$\text{abundance:} \quad \log(\text{ind.}) = \log((\text{ind. * 1000 m}^{-3}\text{)}+1).$$

The biomass concentration and abundances of the mesozooplankton inside and outside the filament were then compared by independent two-sample t-tests at a 95 % confidence interval and unequal variances.

Since the different size fractions and zooplankton groups, respectively, were not sampled independently, the probability were tested simultaneously after an adjustment according to Bonferroni ($n \times p$).

3. Results

3.1. Hydrography

The investigated filament extended about 150 - 200 km off the coast. The cold upwelling water was detected down to a water depth of approx. 100 m and was covered by a warm surface water layer in the upper 15 m (Fig. 5). The water temperature and salinity were measured with the MOCNESS sensors continuously (every 4 seconds) along the longitudinal transect at 10.65 °E on the southern border of the filament between 18.67 °S and 18.85 °S (Fig. 10). For the comparison of inside and outside of the upwelling filament the descending and ascending nets were excluded from data.

Net L2 was conducted in a depth of 66 m, below the thermocline, and thus sampled mainly subsurface water (SSW). Here a temperature of 14.7 °C was detected and salinity dropped sharply to 35.43 PSU. Then water mass 'A' (WMA) was detected between km 3 and km 8 by nets L4 - L7. The transition water (TW) followed between km 7 and km 14. Nets L8, R2 and R3 detected a temperature of 15.7 - 16.2 °C, whereas salinity decreased to the lowest value around 35.52 PSU. At the end of the track up to ~ km 20 the fourth water mass 'B' (WMB) was sampled with the nets R4 - R8, where the temperature increased up to 16.8 °C and salinity was around 35.51 PSU. At the end of the transect salinity and temperature increased again to 35.55 PSU and 16.5 °C.

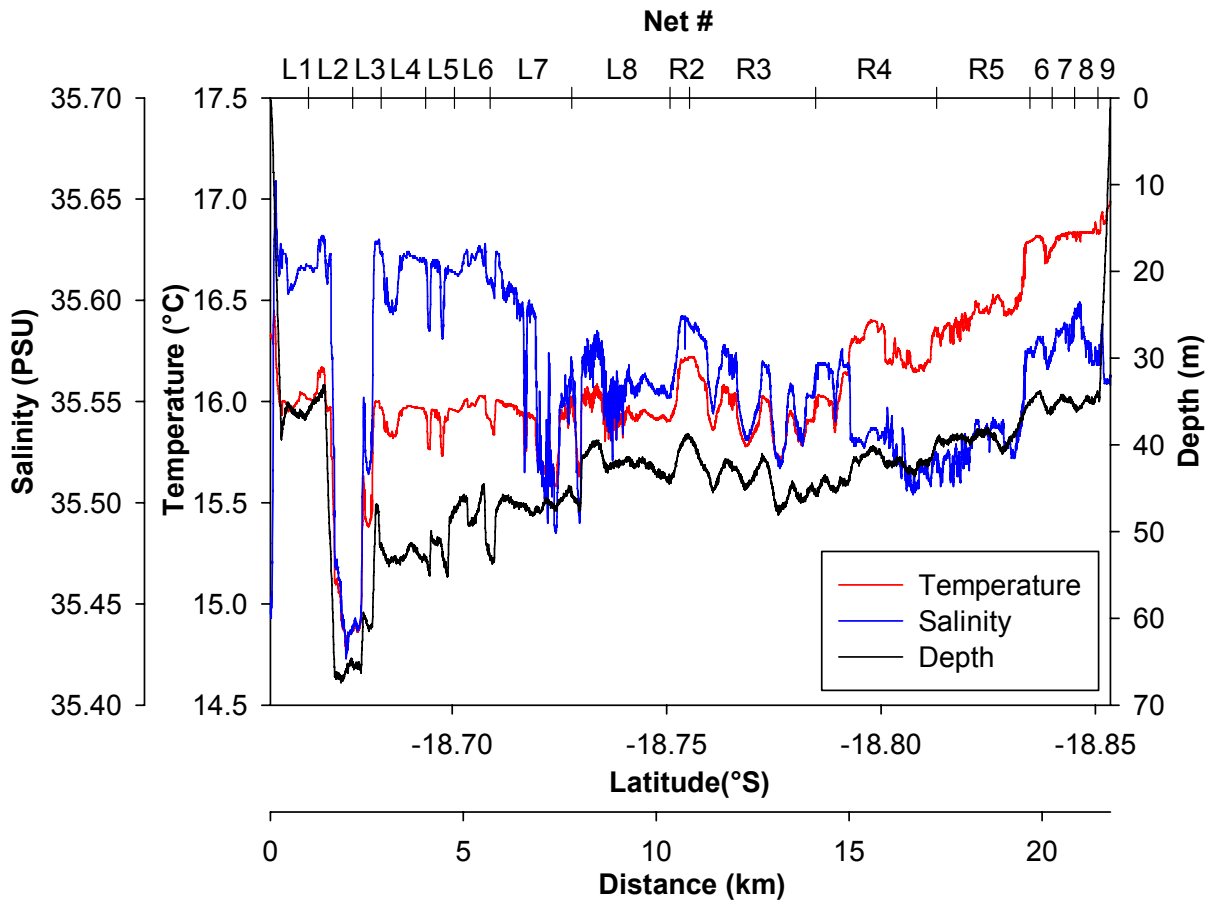


Figure 10: Horizontal profile of water temperature ($^{\circ}\text{C}$) and salinity (PSU) in the Benguela Upwelling system on October 3rd 2010 at latitudes from 18.67°S to 18.85°S along the longitudinal transect at 10.65°E for ~ 22 km.

Based on the investigations of water temperature and salinity four different water masses at the southern border of the filament have been identified (Fig. 11). Generally temperature and salinity showed an opposite pattern. Despite the small-scale variability of temperature and salinity, which is correlated with changes in sampling depth, the properties of the four water masses were distinctly different.

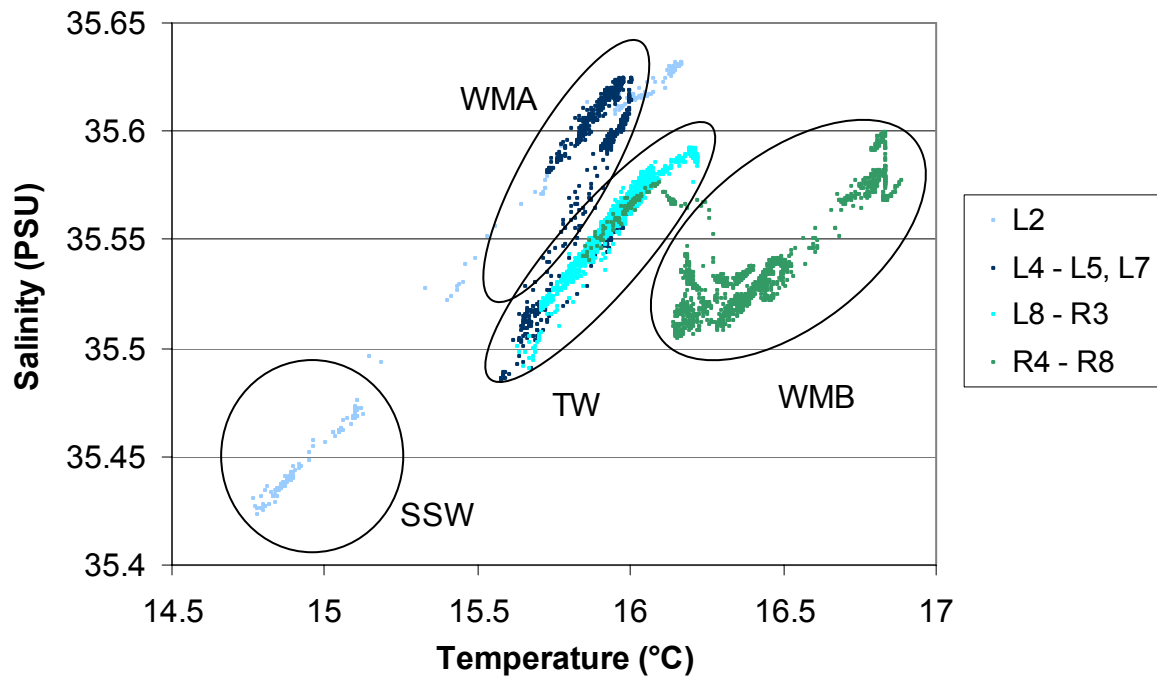


Figure 11: Profile of water temperature (°C) and salinity (PSU) of the MOCNESS haul in subsurface water (SSW), water mass 'A' (WMA), transition water (TW), and water mass 'B' (WMB).

3.2. Distribution of Biomass

The lowest biomass concentration ($6714 \text{ mg} \cdot 1000 \text{ m}^{-3}$) for the sum of fractions $\leq 5 \text{ mm}$ was detected in net L2, which sampled mainly subsurface water (SSW) below the thermocline (Fig. 12). The very low value for the biomass coincides with the drop in temperature and salinity. A higher value ($27710 \text{ mg} \cdot 1000 \text{ m}^{-3}$) for the sum of fractions $\leq 5 \text{ mm}$ was detected for water mass 'A' (WMA), which was conducted by nets L4 - L7. Also in the transition zone (TW) a higher biomass ($44546 \text{ mg} \cdot 1000 \text{ m}^{-3}$) has been recorded by nets L8 - R3. The highest concentration ($67753 \text{ mg} \cdot 1000 \text{ m}^{-3}$) for the sum of fractions $\leq 5 \text{ mm}$ was recorded in water mass 'B' (WMB). The biomass concentrations (sum of all sieve fractions $\leq 5 \text{ mm}$) were significantly different ($p = 0.008$) in WMA and WMB. Significant differences for the biomasses of the single sieve fractions were not detected by t-test after an adjustment of the probabilities according to Bonferroni (Tab. 5).

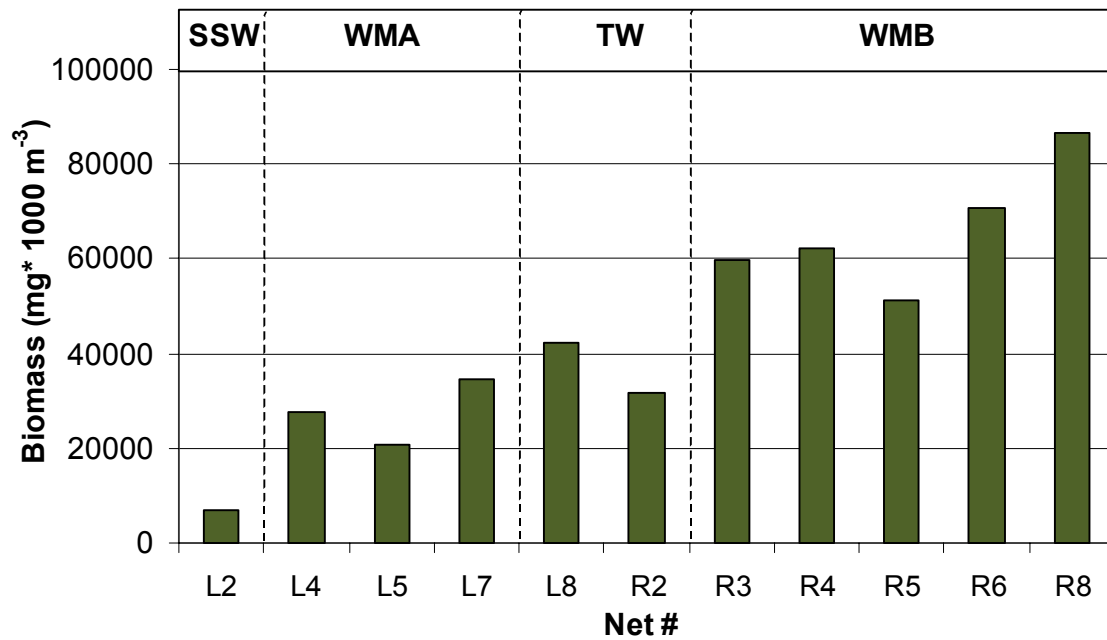


Figure 12: Biomass concentrations for the MOCNESS nets (sum of size fractions ≤ 5 mm) in subsurface water (SSW), water mass 'A' (WMA), transition water (TW), and water mass 'B' (WMB).

Table 5: Biomass concentrations expressed as wet weight ($\text{mg} \cdot 1000 \text{ m}^{-3}$) in subsurface water (SSW: L2), water mass 'A' (WMA: L4, L5, L7), transition water (TW: L8, R2, R3), and water mass 'B' (WMB: R4, R6, R8). P-values of simultaneous t-test for the single fractions after an adjustment according to *Bonferroni*

Fraction (mm)	Biomass ($\text{mg} \cdot 1000 \text{ m}^{-3}$)				t-test
	SSW	WMA	TW	WMB	p-value
< 0.5	411.42	1397.28	1170.04	2246.15	0.887
0.5 - 1	1731.32	3715.72	3544.92	7766.73	0.057
1 - 2	1867.34	6899.18	11074.96	21386.23	0.197
2 - 5	2703.61	15697.50	28756.07	36353.81	0.461
Sum ≤ 5	6713.69	27709.67	44545.99	67752.91	0.008

The composition of the different size fractions of the zooplankton biomass (< 0.5, 0.5 - 1, 1 - 2, and 2 - 5 mm) showed a similar pattern for the four different water masses (SSW, WMA, TW, and WMB, Fig. 13). The biggest size fraction (2 - 5 mm) dominated the zooplankton independently of the different water masses.

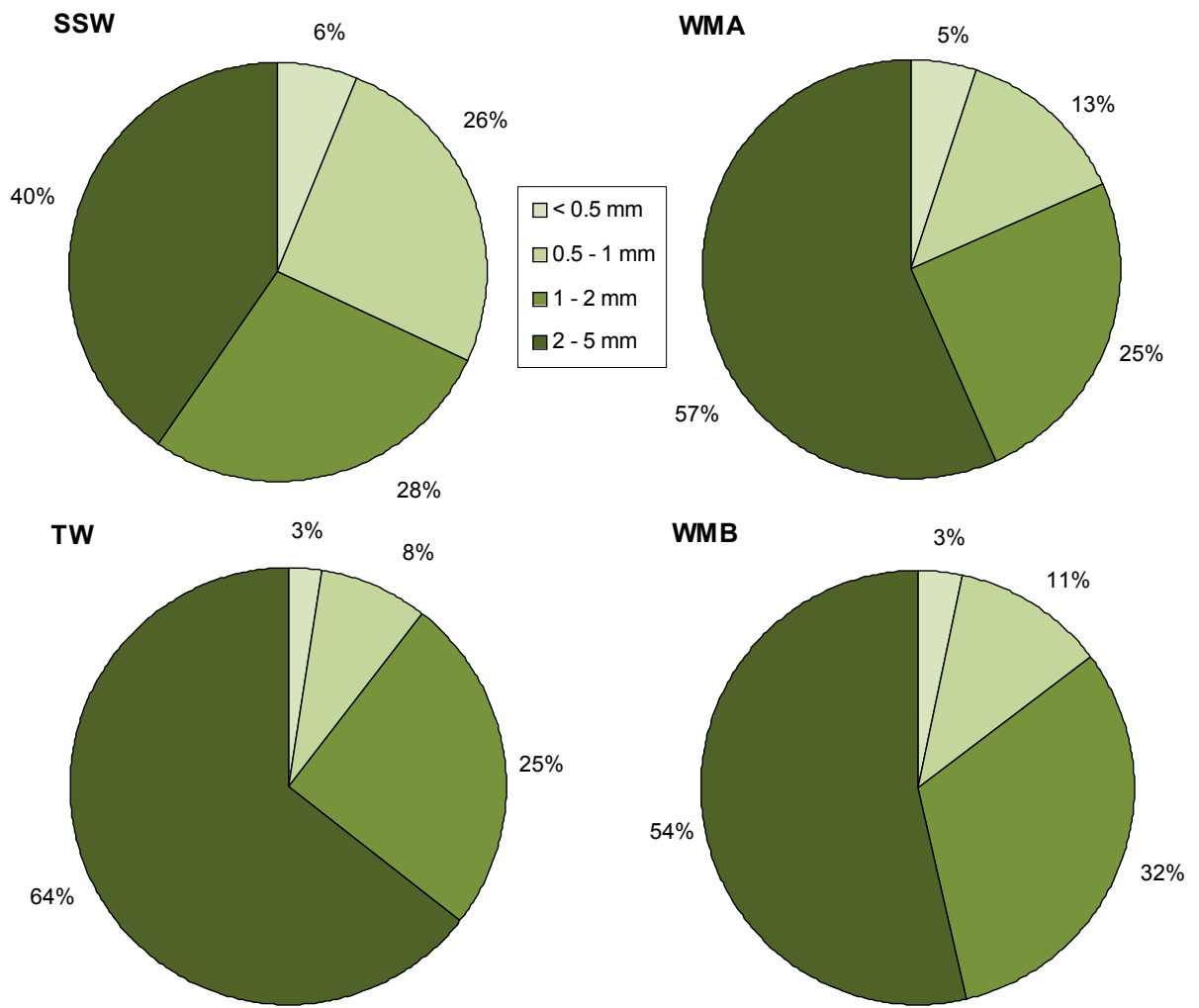


Figure 13: Composition of zooplankton biomass in the different size fractions in subsurface water (SSW: L2), water mass 'A' (WMA: L4, L5, L7), transition water (TW: L8, R2, R3), and water mass 'B' (WMB: R4, R6, R8).

3.3. Distribution of zooplankton

To compare the zooplankton composition of the different water masses the zooplankton abundance for three nets of WMA (L4, L5, L7) and three nets of WMB (R4, R6, R8) were investigated. Sample of net L2, belonging to the subsurface water (SSW), and net L8, which is identified as transition water (TW), were not included in the following statistical comparison.

Like for the biomass, the highest numbers of zooplankton (92368 - 116587 ind. * 1000 m⁻³) for the sum of fractions ≤ 5 mm were detected in WMB, compared to WMA and TW (Fig. 14). Mean zooplankton abundance for the sum of fractions ≤ 5 mm in WMB (103306 ind. * 1000 m⁻³) was 5.8 times higher than in WMA (17954 ind. * 1000 m⁻³). The t-test for the abundances showed a significant difference (p = 0.004) between these water masses (Tab. 6). Single sieve fractions of WMA and WMB did not indicate significant differences.

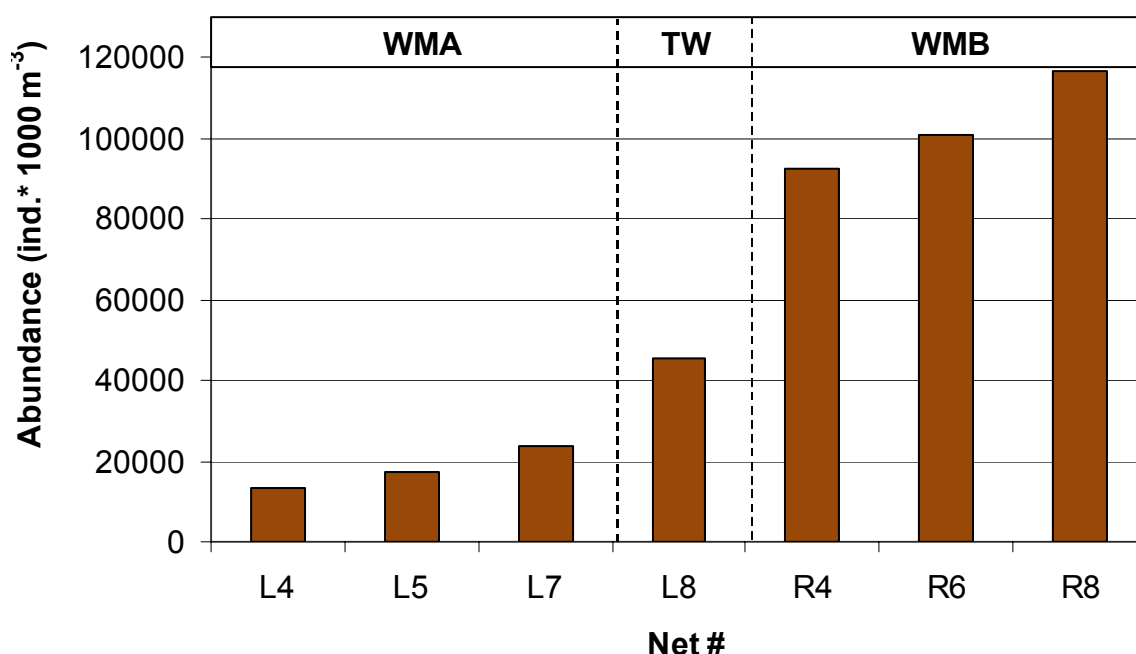


Figure 14: Abundances of the zooplankton in the MOCNESS nets (sum of size fractions ≤ 5 mm) in subsurface water (SSW), water mass 'A' (WMA), transition water (TW), and water mass 'B' (WMB).

Table 6: Abundances of the zooplankton expressed as individuals * 1000 m⁻³ (sum of size fractions ≤ 5 mm) in water mass 'A' (WMA: L4, L5, L7) and water mass 'B' (WMB: R4, R6, R8). P-values of simultaneous t-test for the single fractions after an adjustment according to *Bonferroni*.

Fraction (mm)	Abundance (ind. * 1000 m ⁻³)		t-test
	WMA	WMB	p-value
< 0.5	599.6	13832.2	0.391
0.5 - 1	6237.1	29739.4	0.104
1 - 2	6262.4	36393.7	0.167
2 - 5	4854.7	23341.0	0.666
Sum ≤ 5	17953.7	103306.3	0.004

The composition of the zooplankton size fractions showed a similar pattern in both water masses (WMA and WMB). Middle-size and large zooplankton occurred dominantly in WMA and WMB, respectively (Fig. 15). Exceptionally, the relative abundance of zooplankton in the sieve fraction < 0.5 mm increased from 3 % in WMA to 13 % in WMB. The relative importance increased by a factor of 23, nevertheless no significant difference (p = 0.391) with a probability adjusted according to Bonferroni was recorded.

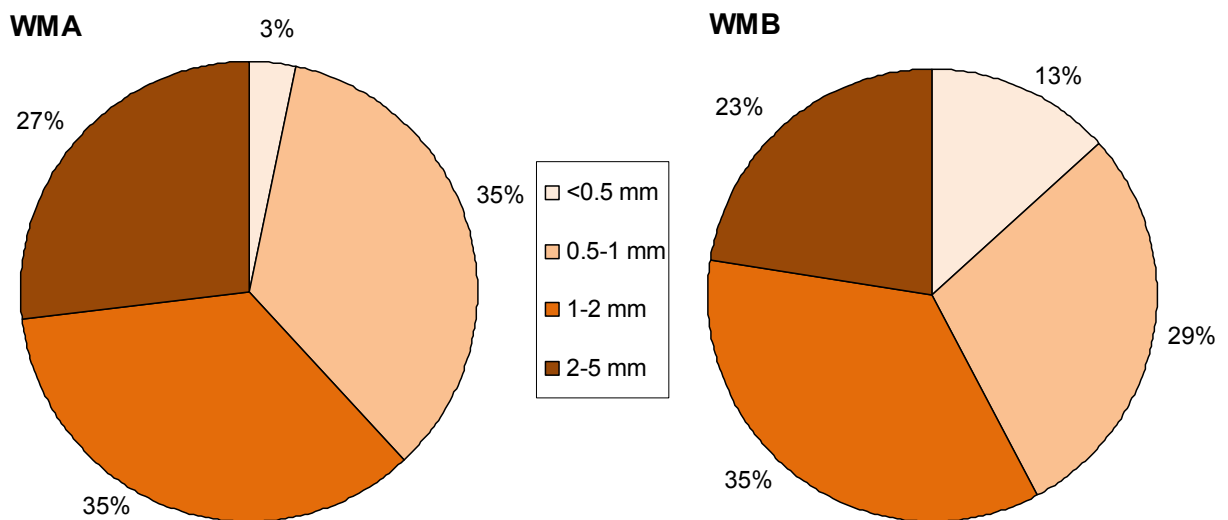


Figure 15: Composition of zooplankton abundance for the different size fractions in water mass 'A' (WMA: L4, L5, L7) and water mass 'B' (WMB: R4, R6, R8).

For the determination of the two different water masses WMA (L4, L5, L7) and WMB (R4, R6, R8) the taxonomical composition of the mesozooplankton was investigated. The numerical and relative abundance of all taxa are shown in table 7. The zooplankton community are excluding Siphonophora, exuviae, and carcasses.

The Crustacea dominated the zooplankton (sum of size fractions ≤ 5 mm) with more than 90 % (Tab. 7) and showed statistically significant difference ($p = 0.017$) between the water masses. In WMA 73.0 % whereas in WMB 82.0 % of Crustacea belonged to the Copepoda. Therefore significant difference of the abundance ($p = 0.018$) was detected. As for the total zooplankton the mean abundance of Copepoda was 6.5 times higher in WMB (84677 ind. $\cdot 1000$ m⁻³) compared to WMA (13102 ind. $\cdot 1000$ m⁻³, Fig. 16). Within the Copepoda, there was a shift to a higher relative importance of Cyclopoida (mainly *Poecilostomatoida*) from WMB (13.2 %) to WMA (1.7 %), although this was not statistically significant ($p = 0.102$).

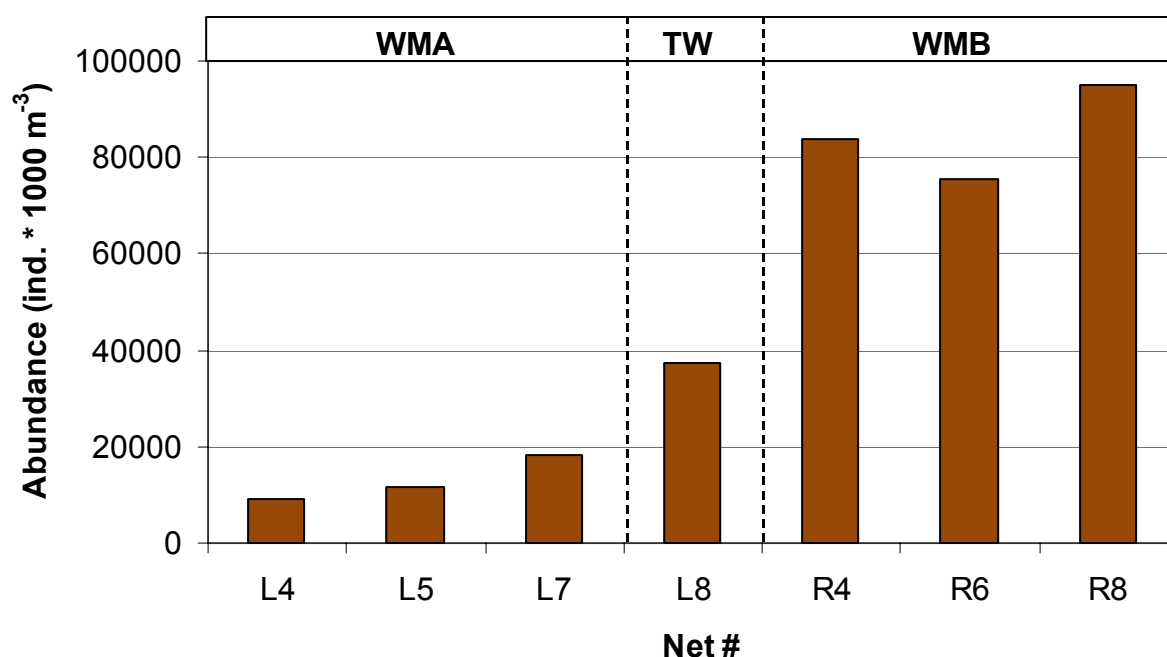


Figure 16: Abundances of Copepoda in the MOCNESS nets (sum of size fractions ≤ 5 mm) in water mass 'A' (WMA: L4, L5, L7), transition water (TW: L8, R2, R3), and water mass 'B' (WMB: R4, R6, R8).

Table 7: Numerical and relative abundances in the MOCNESS nets (sum of size fractions ≤ 5 mm) in water mass 'A' (WMA: L4, L5, L7) and water mass 'B' (WMB: R4, R6, R8). P-values of simultaneous t-tests for the abundances were adjusted according to *Bonferroni*. (N / A) p-values could not be determined due to zero values.

Taxon	Abundance in WMA (ind. * 1000 m ⁻³)	Relative Abundance in WMA (%)	Abundance in WMB (ind. * 1000 m ⁻³)	Relative Abundance in WMB (%)	t-test p-value
Total zooplankton	17953.7	100.00	103306.3	100.00	0.004
Crustacea	16706.3	93.05	97264.8	94.15	0.017
Copepoda	13101.5	72.97	84676.6	81.97	0.018
Copepoda Calanoida	12789.1	71.23	71012.6	68.74	0.010
Copepoda Cyclopoida	312.4	1.74	13664.0	13.23	0.102
Malacostraca & Crustacea Larvae	3441.6	19.17	9614.5	9.31	0.201
Euphausiacea	1151.7	6.41	3063.2	2.97	0.188
Decapoda, Mysidacea & Crustacea larvae	1785.0	9.94	5699.5	5.52	0.422
Amphipoda	504.9	2.81	851.8	0.82	0.430
Ostracoda	163.2	0.91	2973.7	2.88	0.097
Gelatinous	1192.9	6.64	5791.8	5.61	0.260
Semi-Gel. Organisms	1190.9	6.63	5791.8	5.61	0.130
Mollusca	287.9	1.60	3378.6	3.27	0.370
Chaetognatha	616.8	3.44	1684.2	1.63	0.399
Polychaeta	286.1	1.59	729.0	0.71	0.747
Gelatinous Organisms	2.0	0.01	0.0	0.00	N / A
Fish	14.7	0.08	160.7	0.16	0.451
Fish larvae	4.1	0.02	160.7	0.16	0.055
Fish eggs	10.6	0.06	0.0	0.00	N / A
Undefined	39.7	0.22	89.0	0.09	1.000

The abundance of Ostracoda was higher (2974 ind. * 1000 m⁻³) in WMB than in WMA (163 ind. * 1000 m⁻³), but the relative importance increased from 0.9 % in WMA to 2.9 % in WMB. A significant difference could not be detected (p = 0.097).

The Chaetognatha occurred in higher relative abundance on WMA (3.4 %) compared to WMB (1.6 %). However, the numerical abundance in WMB (1684 ind. * 1000 m⁻³) was higher than in WMA (617 ind. * 1000 m⁻³). The Chaetognatha were dominantly in the size fraction 2 - 5 mm in WMA with 42 % and in WMB with 54 % (Fig. 17 A), but no statistical difference between the two water masses (p = 0.193, Tab. A.10) was detected.

The concentration of Malacostraca and Crustacea larvae was higher in WMB (9615 ind. * 1000 m⁻³) than in WMA (3442 ind. * 1000 m⁻³), although the relative abundance decreased from 9 % in WMB to 19 % in WMA. A significant difference in the abundances was not detected (p = 0.201). Within the Malacostraca, Euphausiacea also showed a higher abundance in WMA (6.4 %) than in WMB (3.0 %), but the corresponding t-test did not show a significant difference (p = 0.188). Euphausiacea occurred in highest relative abundance in size fraction 2 - 5 mm in WMA (67 %) and WMB (77 %), respectively (Fig. 17 B), but with no significant difference between the two water masses (p = 0.174, Tab. A.11)

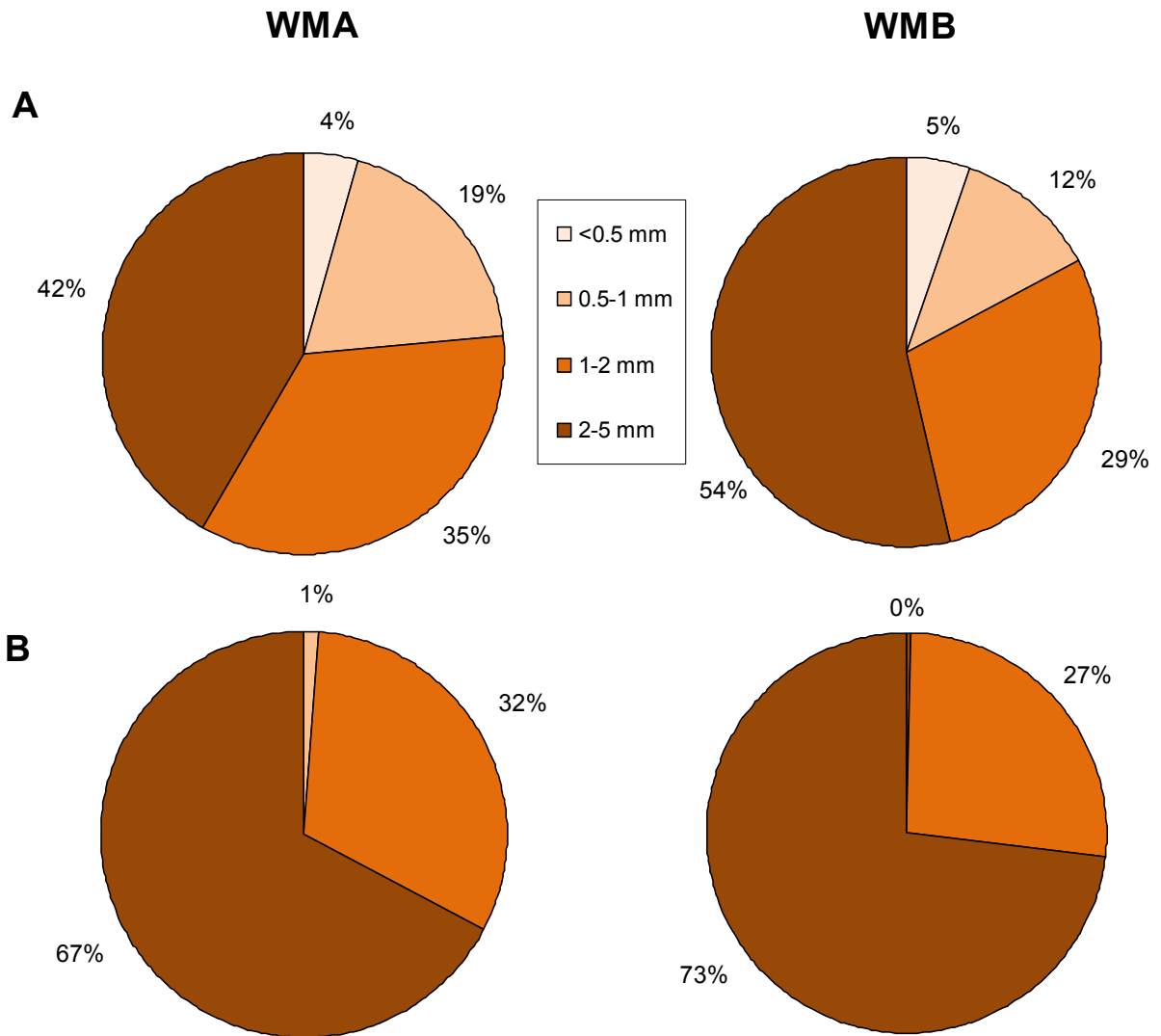


Figure 17: Composition of (A) Chaetognatha and (B) Euphausiacea abundances of the different size fractions in water mass 'A' (WMA: L4, L5, L7) and water mass 'B' (WMB: R4, R6, R8).

In the following table 8 all groups with a relative abundance > 1 % are shown, distinguish from the dominance in WMA or WMB. The Euphausiacea, Amphipoda, Chaetognatha, Malacostraca, and Crustacea larvae changed from a dominance of numerical abundance in WMB to a dominance in WMA with regard to the relative importance.

Table 8: Dominance (+) of taxa with relative abundance > 1 % in water mass 'A' (WMA: L4, L5, L7) or water mass 'B' (WMB: R4, R6, R8).

Taxon	Dominance in	
	WMA	WMB
Copepoda Calanoida	+	-
Copepoda Cyclopoida (mainly <i>Poecilostomatoida</i>)	-	+
Euphausiacea	+	-
Malacostraca & Crustacea larvae	+	-
Amphipoda	+	-
Ostracoda	-	+
Mollusca (mainly Pteropoda)	-	+
Chaetognatha	+	-

The Mollusca was the only group, beside Copepoda Calanoida and Ostracoda, that occurred in higher relative numbers in WMB compared to WMA (Tab. 8). Mainly Pteropoda were recorded within the Mollusca. The relative abundance was 2 times higher in WMB (3.3 %) than in WMA (1.6 %). However, the t-test did not show significant differences for the Mollusca abundance ($p = 0.370$) between the two water masses.

The performed t-test for the fish abundance showed no significant difference ($p = 0.451$), probably because the organisms occurred in very small numbers in both water masses. In WMA the numbers of fish larvae and eggs reached 15 ind. * 1000 m⁻³, where in WMB 160 ind. * 1000 m⁻³ occurred, which constitutes < 0.2 % of total zooplankton abundance in both water masses.

Despite the Siphonophora were excluded from the total mesozooplankton, they appeared to predominate the WMB with significant difference ($p = 0.043$). The numerical abundance in the sum of fractions ≤ 5 mm reached 1381 ind. * 1000 m⁻³ in WMB compared to 20 ind. * 1000 m⁻³ in WMA. The relative abundance increased from 0.1 % in WMA to 1.3 % in WMB. Further the abundance of exuviae and carcasses was detected, but not included in the total zooplankton community. The numerical abundance did not show a significant

difference ($p = 0.631$) of the abundance in the different in WMA (8855 ind. * 1000 m⁻³) and WMB (7560 ind. * 1000 m⁻³). However, the relative numbers increased by a factor of 6.8 from 7.3 % in WMB to 49.3 % in WMA.

In summary, most of the numerical abundances were higher in WMB, compared to WMA. Statistically significant differences for groups, which were detected in higher relative numbers in WMA, were recorded for Copepoda Calanoida within the Crustacea. However, the Cyclopoida (mainly *Poecilostomatoida*), Mollusca (mainly Pteropoda), and Ostracoda occurred in higher relative numbers in WMB, but with no statistically difference.

4. Discussion

4.1. Hydrographical characterisation

Upwelling regions are characterised by cold upwelling nutrient rich deep water and result from surface water currents, which in turn are induced by the major wind fields. These upwelling structures are only built in eastern boundary currents at the edge of the ocean. The four major ocean currents are the Humboldt Current System (Gibson et al. 2007), the California Upwelling region (Lynn & Simpson 1987), the NW African Upwelling region (Hernandez-Guerra et al. 2002), and the Benguela Current (Garzoli & Gordon 1996). The northern Benguela Upwelling system off Namibia is characterised by its strong seasonality and therefore creates good facilities for the formation of filaments (Campillo-Campbell & Gordo 2001). The upwelling filaments may extend several hundred kilometres offshore.

In October 2010, during the cruise 356 of RRS (Royal Research Ship) Discovery, within the GENUS project (Geochemistry and Ecology of the Namibian Upwelling System) in the northern Benguela, an upwelling filament was intensively investigated by oceanographers on board. Unfortunately, the zooplankton sampling for this thesis was not conducted simultaneously with the oceanographic measurements and furthermore took place at other stations.

To determine the abiotic parameters of the investigated filament sensors of the MOCNESS device were used. Based on these results, four distinct water masses were identified: the subsurface water (SSW), water mass 'A' (WMA), the transition water (TW), and water mass 'B' (WMB). The temperature of the colder WMA was 1.5 °C lower than the surrounding water, which is characterising for the inside of upwelling filaments (Keister et al. 2008). Consequently the higher temperatures of WMB indicated offshore water. However, salinity showed an opposite pattern with lower values in WMB than in WMA, even though the inside of upwelling filaments is typically characterised by its low salinity concentration (Keister et al. 2008).

This makes it difficult to determine the two water masses (WMA and WMB) distinctly as 'inside' and 'outside' of the filament. Still, transition water (TW) and subsurface water (SSW) did not build part of the filament structure. Boyd and Agenbag (1985) described a saline water type (35.3 - 35.5 PSU) with a temperature lower than 15 °C in upwelling system off central Namibia in autumn. The authors suggested that it might have been upwelling water from more northern or offshore sources. The biological data of this study may help to interpret the recorded patterns for the identification of the filament structure.

4.2. Biological characterisation

In the northern Benguela Current region off Namibia zooplankton occur in low species diversity but high abundances (Shannon & Pillar 1986), possibly due to the intense upwelling and therewith irregularities in temperature and salinity (Sakko 1998). Upwelling causes changes in the physical conditions such as colder temperatures and lower salinities, and chemical environment like increased availability of nutrients (Keister et al. 2008). This is followed by a shift in the phytoplankton community towards large diatoms (Margalef 1962, Mitchell-Innes & Walker 1991). Also, in the investigated Benguela Current system diatoms appeared to predominate the phytoplankton community. With their high nutrient requirements, diatoms are adapted to the turbulent conditions of the upwelling system (Shannon & Pillar 1986). They are mainly eaten by Copepoda and Euphausiacea (Loick et al. 2005).

The Benguela region is characterised by the presence of cool water and high biological productivity (Sakko 1998). Timonin et al. (1992) published that the zooplankton biomass is closely related to changes in upwelling intensity in the northern Benguela ecosystem. For eastern boundary currents filaments are common and may transport produced zooplankton into offshore direction. This can result in significantly (> 10 times) higher values within an upwelling filament compared to the offshore water (Fig. 18, Keister et al. 2008). Escribano and Hidalgo (2000) recorded higher numerical abundances of Copepoda (Fig. 19) related to an upwelling system. Upwelling activity in their study was detected by lower water temperatures ($17.5\text{ }^{\circ}\text{C}$) inside compared to higher values outside of the current ($20.5\text{ }^{\circ}\text{C}$).

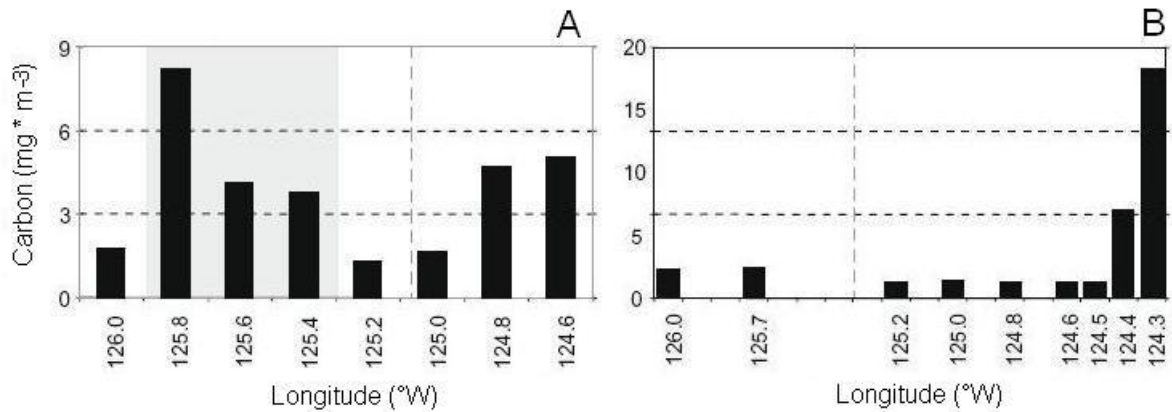


Figure 18: Biomass of Copepoda, when upwelling filament was (A) present at $42.7\text{ }^{\circ}\text{N}$ and (B) absent $41.9\text{ }^{\circ}\text{N}$ off Oregon in USA in August 2002. Concentrations are labelled with their longitudes. Grey highlighting indicate stations within cold filaments, vertical dashed lines show the location of the upwelling front; after Keister et al. (2008).

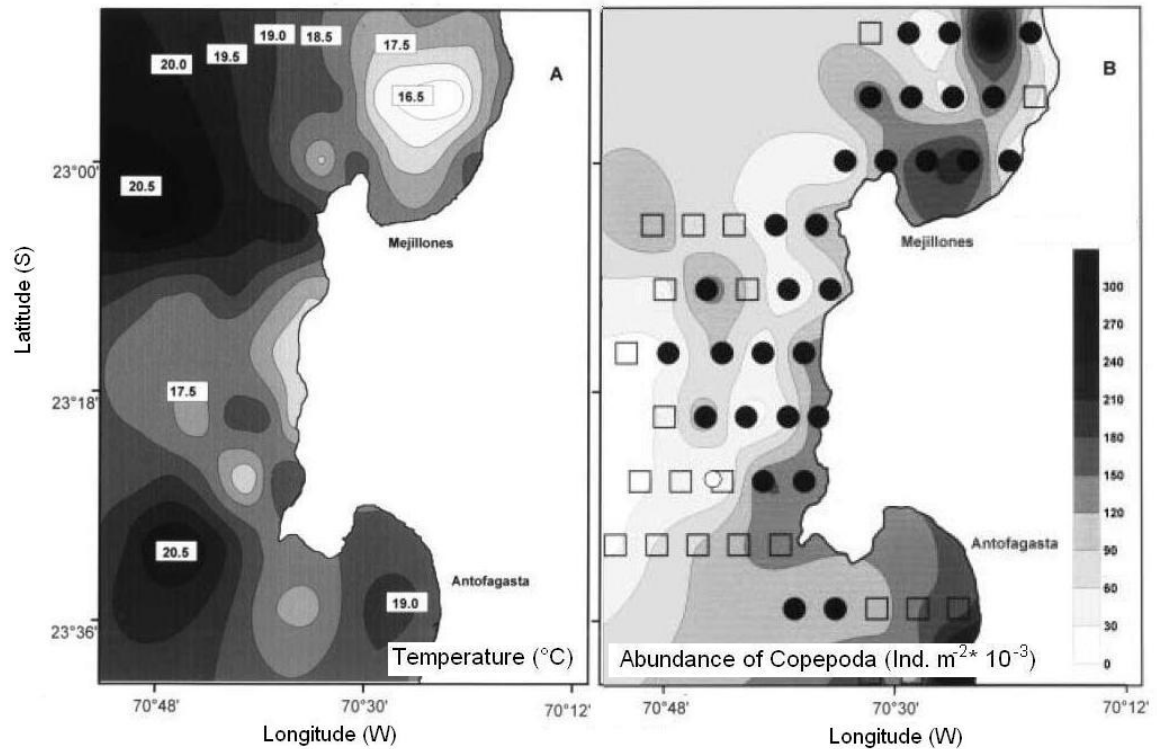


Figure 19: (A) Upwelling activity recorded by sea surface temperature ($^{\circ}\text{C}$) and (B) spatial abundance of Copepoda ($\text{ind. m}^{-2} * 10^{-3}$) at Mejillones Peninsula in Chile (23.3°S , 70.6°W) in December 1996. Filled circles represent locations, that were grouped as belonging to upwelling-type conditions, open squares are non-upwelling type locations determined water temperature; after Escribano & Hidalgo (2000).

The Chaetognatha and Euphausiacea occurred dominantly in the largest size fraction (2 - 5 mm). The relative importance of both group increased from WMA to WMB, whereas the total numerical abundance (sum of all size fractions ≤ 5 mm) increased oppositely from WMB to WMA. Gibbons (1992) investigated larger and sexually more developed Chaetognatha in offshore regions compared to more inshore locations. Further Barange and Stuart (1991) recorded larger animals of Euphausiacea offshore with more spermatophores. These conclusions coincide with the higher abundance of larger Chaetognatha and Euphausiacea in WMA, which is identified as the outside of the filament and therewith offshore water. This may be account for the observed differences in Copepoda consumption, since they are common preys.

The composition showed that Copepoda Cyclopoida (mainly *Poecilostomatoida*), Ostracoda, and Mollusca (mainly Pteropoda) occurred in higher relative abundances in the warmer WMB than in WMA. These organisms indicate oceanic

water masses (Tseng et al. 2008, Zhaoli & Chunju 2006) and therefore confirms the assumption, that WMB was offshore water.

Altogether, in this thesis, the hydrographical analysis and the preliminary results of the zooplankton composition identify the warmer water mass 'B' as outside and the colder water mass 'A' as inside of the filament. Nevertheless, the hypothesis of enhanced stocks within an upwelling filament has to be rejected by these results. Possible reasons regarding the unexpected distribution will be discussed below.

- The lower biomass and abundances of zooplankton in WMA could be caused by predation pressure. Copepoda were the most abundant and diverse group of the zooplankton community in both sampled water masses (WMA and WMB). The Copepoda are important prey for many organisms and may have attracted predators, which then increased in abundance, such as Chaetognatha (Purcell 2003, Sabates et al. 2010, Raskoff 2002, Øresland 2000, Gibbons et al. 1992), also found in higher relative abundance in WMA. Consequently, the decrease in numbers of predominant Copepoda and the generally lower zooplankton abundance in WMA could be due to predation. The Lotka-Volterra model describes such typical interactions between prey and predators (Fig. 21) by assuming a set of the following four fixed positive constants: growth rate of prey (A), mortality of prey (B), mortality of predators (C), and growth of predators (D). The model describes the dynamic of growth and decline, where predators thrive with higher rate of prey and decreases again when prey population gets lower as a result of predation pressure. This is followed by another peak in abundance of prey and is then repeated (Fig. 20). The prey population (x, red line) increases at a rate $dx = A x dt$ whereby the predator population (y, blue line) decreases at a rate $dy = -C y dt$. To investigate whether the zooplankton abundances of the filament in this thesis was decreased by top-down control, it would be necessary to differentiate between the abundances of prey and predators on a larger temporal scale.

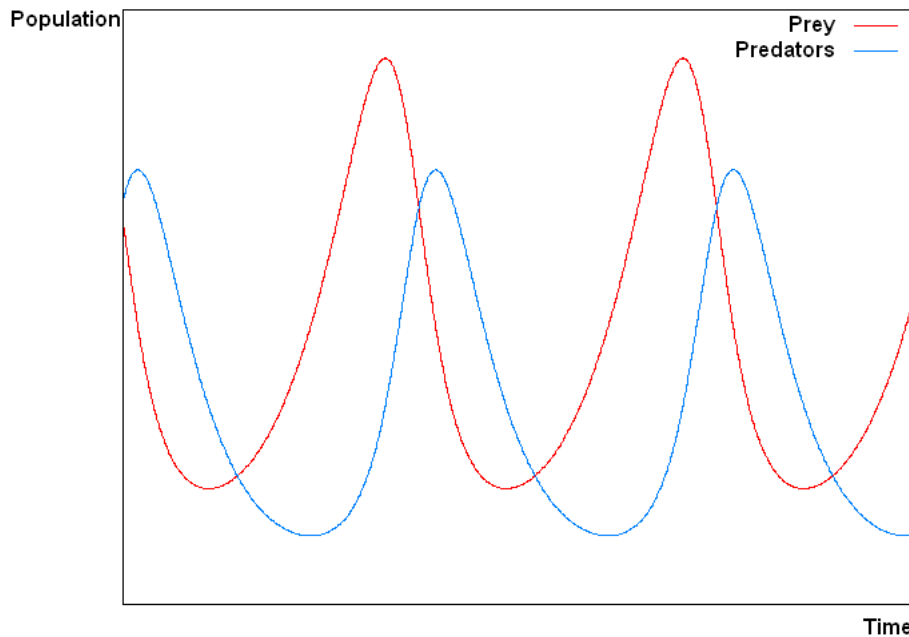


Figure 20: The model system of Lotka-Volterra with periodic populations of prey (red line) and predators (blue line).

- One may speculate that diel vertical migration (DVM) has caused the differences between the water masses. DVM of zooplankton and micronekton organisms is very prominent in oceanic waters (Cornejo & Koppelman 2006). The animals reside in deeper waters during daytime (e.g. to avoid predators in the darkness) and move to the surface for feeding during daytime (see Robinson et al. 2010). This behaviour is mainly performed by Copepoda species like *Metridia* and *Pleuromamma* (Weikert & Koppelman 1993), Euphausiacea (Brown et al. 1979, Komaki 1967), and myctophid fishes (Cornejo & Koppelman 2006). Commencement of sampling for this study was at night, fifteen minutes after sunset, so the colder water mass 'A' initiated by net L4 at 17:59 UTC was already sampled in full darkness. Therefore, diel vertical migration as a reason for the differences in abundance between the water masses is unlikely.
- The Ekman transport causes drifts of cold upwelling water offshore (see Introduction) and exports zooplankton biomass off the coast. Hansen et al. (2005) mentioned a decrease in abundance of all Copepoda species in September 2000 during the highest upwelling activity, which may result

from Ekman offshore transport (Kruger & Boyd 1984). Also during the years 1973 and 1982 (August - October), when strongest upwelling was recorded and temperatures were lowest, a minimum of zooplankton abundance was detected (Visser et al. 1973, Le Clus & Kruger 1982). It is also possible that zooplankton were transported out of the filament water from WMA into WMB by subsurface Ekman drift.

- The abundance of zooplankton appears to be commonly linked to chlorophyll-*a* concentration (Fig. 21). Although higher chl-*a* concentrations normally occur with colder upwelling water (Escribano 2000, Cravo et al. 2010), higher chl-*a* fluorescence in the warmer water mass (WMB) was detected in other experiments related to this thesis (Muller, unpublished results). This may show that the dispersion of chl-*a* concentration is not necessarily equal in all upwelling filaments. Thus, the higher biomass and abundances of zooplankton in the WMB could be due to the higher chl-*a* concentration since it plays an important role to initiate the zooplankton reproduction.

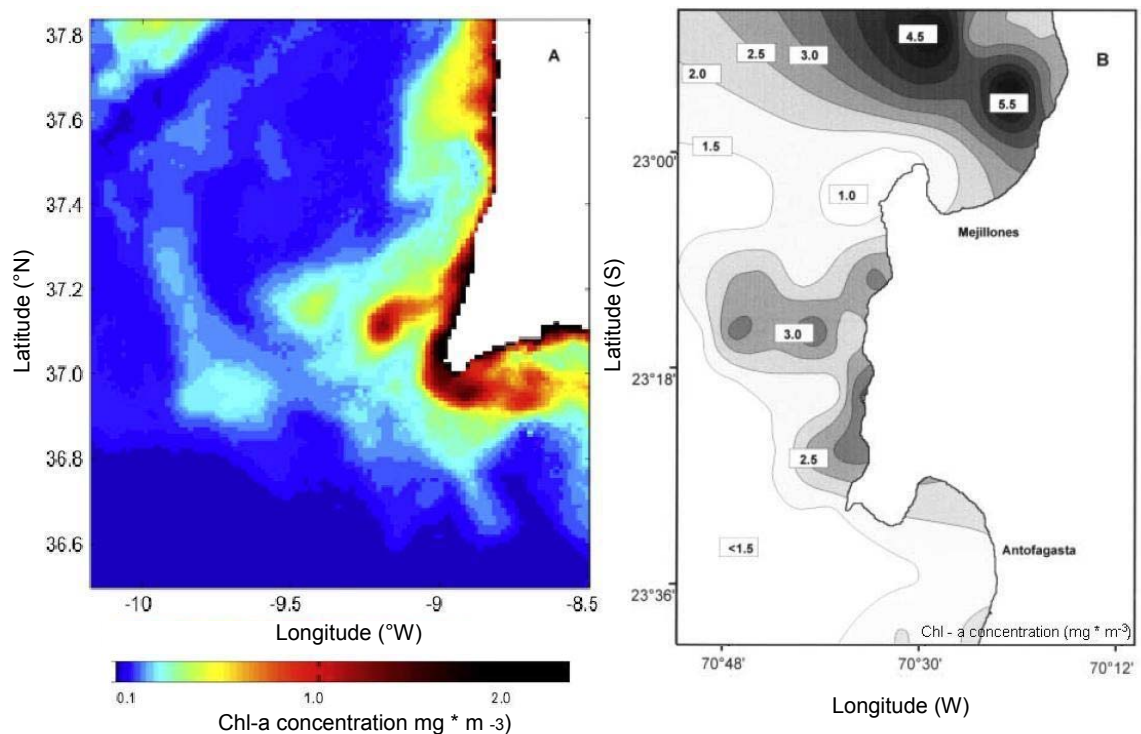


Figure 21: Chlorophyll-*a* concentration related to upwelling activity off (A) Portugal; after Cravo et al. (2010) and (B) Chile; after Escribano & Hidalgo (2000).

- Since the relative number of exuviae and carcasses considerably increased inside the filament water, in WMA, substantial mortality and sinking of the zooplankton out of the filament can be a reason for the decreased total zooplankton community.
- The extreme instability of upwelling systems can result in other currents, additionally to the Ekman transport, such as downstream eddies and opposite direction currents (Wroblewski 1980, 1882, Peterson et al. 1997). These features can export the zooplankton biomass via recirculation inshore or into deeper oceanic water layers and may have caused the decrease of abundance in WMA. Further riverine outflows with high nutrient inputs and frontal borders, which are not permeable for nutrients (Agostini & Bakun 2002) may have been involved in the changes of environment of the filament.

In conclusion, one single cause or the combination of several factors may have delivered the unexpected results of this thesis. Since upwelling regions are dynamic systems, they can be influenced by different oceanic water structures, which results in shift of the characteristic parameters. The upwelling process may be affected by small-scale spatial downwelling structures or eddies, which initiate the return of produced zooplankton. Further, the biomass can be entrained out of the filament by biological scenarios like mortality or sinking of the biomass. Finally, replicated investigations on the environmental patchiness in upwelling systems will be necessary to solve the problem. Unfortunately such investigations are beyond the time-frame of this thesis.

4.3. Critical evaluation of methods

One of the major gaps of this study is the shift in time between hydrographical and biological measurements. Generally, for the investigation of the mesozooplankton distribution in upwelling filaments, it would be necessary to take replicas at different times and locations simultaneously with the measurements of the abiotic parameters.

Instead of a more precise dry weight determination, wet weighing was chosen to allow subsequent taxonomical analyses of the samples. Wet weighing is less accurate, because interstitial water remains between the organisms. To increase the scientific value of the study subsamples should have been investigated to gain a higher taxonomical resolution. Larger organisms (> 5 mm) were unfortunately not quantitatively sampled by the MOCNESS-nets with a mesh size of 333 μm , and thus are not included evaluated data.

According to scientific standards it would be desirable to generate research project sustainably on fundamental research of replicas and evolve hypothesis driven research designs. Still practice-oriented projects as the present study supply valuable results and provide suggestions for future investigations.

4.4. Outlook

Upwelling filaments typically stay for a few days, thus a schedule must be performed just on time. Future investigations should optimally begin at the time of occurrence of an upwelling filament until it disappears again. Therefore attention should be paid during the investigation by oceanographical measurements via SST, for the identification of upwelling filaments. Then gears should be applied, which allow a fast resolution of the abiotic and biotic parameters in the water column, like a SCANFISH (see Introduction).

Furthermore, periodical analyses throughout a year would obtain results about the process of filaments in different seasons to require characterisations of during different times of the year. Sampling should be located at the northern and southern border of a filament with several vertical and horizontal hauls to receive greater data set of the mesozooplankton diversity. Additional analyses of characteristic key species for the inshore and offshore water could determined. Moreover, future projects could include analyses, which deal with the sexually development and a growth model for each group of the zooplankton, since high primary production inside of an upwelling filament initiate higher reproduction rates, and thus higher abundances of larvae and eggs.

References

- AGOSTINI V.N. and BAKUN A. 2002, 'Ocean triads' in the Mediterranean Sea: Physical mechanisms potentially structuring reproductive habitat suitability (with example application to European anchovy, *Engraulis encrasicolus*). *Fisheries Oceanography* 11, 129-142.
- BARANGE M. and STUART V. 1991, Distribution patterns, abundance and population dynamics of the euphausiids *Nyctiphanes capensis* and *Euphausia hanseni* in the northern Benguela upwelling system. *Marine Biology* 109, 93-101.
- BIANCHI G., CARPENTER K.E., ROUX J.P., MOLLOY F.J., BOYER D. and BOYER H.J. 1999, Field Guide to the Living Marine Resources of Namibia. FAO Species Identification Guide for Fishery Purposes 2, 265 pp.
- BROWN R.G.B., BARKER S.P. and GASKIN D.E. 1979, Daytime surface swarming by *Meganyctiphanes norvegica* (Crustacea, Euphausiacea) off Brier Island, Bay of Fundy. *Canadian Journal of Zoology* 57, 2285-2291.
- BRUNE A., EMERSON D. and BREZNAK J.A. 1995, The termite gut microflora as an oxygen sink: Microelectrode determination of oxygen and pH gradients in guts of lower and higher termites. *Applied and Environmental Microbiology* 61, 2681-2687.
- BUCHHOLZ F. 2010, Report of cruise D356 RRS Discovery September 10th (Walvis Bay) - 13 October 13th 2010 (Cape Town). http://genus.zmaw.de/fileadmin/user_upload/genus/template/D-356_Cruise_Report.pdf.
- CAMPILLO-CAMPBELL C. and GORDOA A. 2004, Physical and biological variability in the Namibian upwelling system: October 1997 - October 2001. *Deep Sea Research Part II: Topical Studies in Oceanography*, 147-158.

- CORNEJO R. and KOPPELMANN R. 2006, Horizontal and vertical distribution of mesopelagic fishes with special reference to *Vinciguerria lucetia* Garman 1899 (Phosichthyidae: Pisces) in the Humboldt Current region off Peru. *Marine Biology* 149, 1519-1537.
- CRAVO A., RELVAS P., CARDEIRA S., RITA F. MARUREIRA M. and SÁNCHEZ R. 2010, An upwelling filament off southwest Iberia: Effect on the chlorophyll-a and nutrient export. *Continental Shelf Research* 30, 1601-1613.
- CURY P.M. and SHANNON L.J. 2004, Regime shifts in the Benguela ecosystem: facts, theories and hypotheses. *Progress in Oceanography* 60, 223-243.
- ESCRIBANO R. and HIDALGO P. 2000, Spatial distribution of copepods in the north of the Humboldt Current region off Chile during coastal upwelling. *Journal of Marine Biology Association UK* 80, 283-290.
- GARZOLI S.L. and GORDON A.L. 1996, Origins and variability of the Benguela Current. *Journal of Geophysical Research* 101, 897-906.
- GIBBONS M.J. 1992, Diel feeding and vertical migration of *Sagitta serratodentata* Krohn *tasmanica* Thomson (Chaetognatha) in the southern Benguela. *Journal of Plankton Research* 14 (2), 249-259.
- GIBBONS M.J., STUART V. and VERHEYE H.M. 1992, Trophic ecology of carnivorous zooplankton in the Benguela. *South African Journal of Marine Science* 12, 421-437.
- GIBBONS M.J. 1999, An Introduction to the Zooplankton of the Benguela Current region. National Book Publishers, Cape Town, 55pp.
- GIBSON R.N., ATKINSON R.J.A. and GORDON J.D.M. 2007, The Humboldt Current System of northern and central Chile. *Oceanography and Marine Biology, An Annual Review* 45, 195-344.

- HANSEN F.C., CLOETE R.R. and VERHEYE H.M. 2005, Seasonal and spatial variability of dominant copepods along a transect off Walvis Bay (23°S), Namibia. *African Journal of Science* 27 (1), 55-63.
- HERNANDEZ-GUERRA A., MACHIN F., ANTORANZ A., CISNEROS-AGUIRRE J., GORDO C., MARRERODIAZ A., MARTINEZ A., RATSIMANDRESY A., RODRIGUEZ-SANTANA A., SANGRA P., LOPEZ-LAATZEN F., PARRILLA P. and PELEGRI J.L. 2002, Temporal variability of mass transport in the Canary Current. *Deep Sea Research Part II: Topical Studies in Oceanography* 49, 3415-3426.
- HUGGETT J.A., VERHEYE H.M., ESCRIBANO R. and FAIRWEATHER T. 2009, Copepod biomass, size composition and production in the Southern Benguela: spatio-temporal patterns of variation, and comparison with other eastern boundary upwelling systems. *Progress in Oceanography* 83, 197-207.
- KEISTER J.E., COWLES T.J., PETERSON W.T. and MORGAN C.A. 2009. Do upwelling filaments result in predictable biological distributions in coastal upwelling ecosystems? *Progress in Oceanography* 83 (1-4), 303-313.
- KOMAKI Y. 1967, On the surface swarming of Euphausiid crustaceans. *Pacific Science* 21 (4), 433-448.
- KOPPELMANN R. 1990, Vergleichende Untersuchung zu Verteilungsmustern von Zooplankton im Nordostatlantik und in Mittelmeeren der ariden Klimazone (europäisches Mittelmeer und Rotes Meer). Diploma Thesis, University Hamburg, 113pp.
- KOTT P. 1953, Modified whirling apparatus for the subsampling of plankton. *Australian Journal of Marine and Freshwater Research* 4, 387-393.
- KRUGER I. and BOYD A.J. 1984, Investigation into the hydrology and plankton of the surface waters off south-western Africa in ICSEAF Divisions 1.3, 1.4 and

1.5 in 1982 / 83. Collection of Scientific Papers of the International Commission for the Southeast Atlantic Fisheries 11, 109-133.

LE CLUS F. and KRUGER I. 1982, Time and space distribution of temperature, salinity, plankton and fish eggs off South West Africa in 1980 / 81 - a preliminary data report. Collection of Scientific Papers of the International Commission for the Southeast Atlantic Fisheries 9, 121-145.

LOICK N., EKAU W. and VERHEYE H.M. 2005, Water-body preferences of dominant Calanoid Copepod species in the Angola-Benguela frontal zone. South African Journal of Marine Science 27, 597-608.

LYNN R.J. and SIMPSON J.J. 1987, The California Current System: The seasonal variability of its physical characteristics. Journal of Geophysical Research 92, 12947-12966.

MARGLEF R. 1962, Succession in marine populations. Advancing frontiers of Plant Sciences 2, 137-188.

MFMR 1996, Economic performance by fishery. Internal memorandum, Windhoek: Ministry of Fisheries and Marine Resources.

MITCHELL-INNES B.A. and WALKER D.R. 1991, Short-term variability during an Anchor station study in the southern Benguela upwelling system: Phytoplankton production and biomass in relation to species changes. Progress in Oceanography 28, 65-89.

MOTODA S. 1959, Devices of simple plankton apparatus. Memoirs of the Faculty of Fisheries Hokkaido University 7, 73-94.

ØRESLAND V. 2000, Diel feeding of the Chaetognath *Sagitta enflata* in the Zanzibar Channel, Western Indian Ocean. Marine Ecology Progress Series 193, 117-123.

- PETERSON W.T., MILLER C.B. and MYERS A.H. 1979, Zonation and maintainance of copepod populations in the Oregon upwelling zone. Deep-Sea Research 26, 467-494.
- PURCELL J.E. 2003, Predation on zooplankton by large jellyfish (*Aurelia labiata*, *Cyanea capillata*, *Aequorea aequorea*) in Prince William Sound, Alaska. Marine Ecology Progress Series 246, 137-152.
- RASKOFF K.A. 2002, Foraging, prey capture, and gut contents of the mesopelagic Nacromedusa *Solmissus spp.* (Cnidaria Hydrozoa). Marine Biology 141, 1099-1107.
- ROBINSON C., STEINBERG D.K., KOPPELMANN R., ROBINSON B.H., ANDERSON T.R., ARISTEGUI J., CARLSON C.A., FROST J.R., GHIGLIONE J.-F., HERNANDEZ-LEON S., JACKSON J.A., QUEGUINER B., RAGUENEAU O., RASSOULZADEGAN F., TAMBURINE C., TANAKA T., WISHNER K.F. and ZHANG J. 2010, Mesopelagic microbial and metazoan diversity and function - a synthesis. Deep-Sea Research (2) 57, 1504-1518.
- SABATÉS A., PAGÈS F., ATIENZA D., FUENTES V., PURCELL J.E. and GILI J.M. 2010, Planktonic cnidarian distribution and feeding of *Pelagia noctiluca* in the NW Mediterranean Sea. Hydrobiology 645, 153-165.
- SAKKO A.L. 1998, The influence of the Benguela upwelling system on Namibia's marine biodiversity. Biodiversity and Conservation 4, 419-433.
- SHANNON L.V. and PILLAR S.C. 1986, The Benguela ecosystem, Part III. Plankton. Oceanography and Marine Biology, An Annual Review 24, 65-170.
- SMITH P.P.K. and BUSECK P.R. 1982, Carbyne forms of carbon: Do they exist? Science 216, 984-986.

- STEEDMAN H.F. 1976, General and applied data on formaldehyde fixation and preservation of marine zooplankton. Zooplankton fixation and preservation, UNESCO Monographs on Oceanographic Methodology 4, 103-154.
- TIMONIN A.G., ARASHKEVICH E.G., DRITS A.V. and SEMENOVA T.N. 1992, Zooplankton dynamics in the northern Benguela ecosystem, with special reference to the copepod *Calanoides carinatus*. South African Journal of Marine Science 12, 545-560.
- TRANTER D.J. 1962, Zooplankton abundance in Australian waters. Australian Journal of Marine and Freshwater Research 13, 106-142
- TSENG L.C., KUMAR R., DAHMS H.U., CHEN C.T., SOUISSI S., CHEN Q.C. and HWANG J.S. 2008, Copepod community structure over a marine outfall area in the north eastern South China Sea. Journal of the Marine Biological Association of the United Kingdom 88 (5), 955-966.
- VISSER G.A., KRUGER I., COETZEE D.J. and CRAM D.L. 1973, The environment, In Cape Cross Programme (Phase III). Sea Fisheries Branch South Africa, 9 pp.
- WEIKERT H. 1977, Copepod carcasses in the Upwelling region south of Cap Blanc, NW Africa. Marine Biology 42, 351-357.
- WEIKERT H. and KOPPELMANN R. 1993, Vertical structural patterns of deep-living zooplankton in the NE Atlantic, the Levantine Sea and the Red Sea: a comparison. Oceanologica Acta 16, 163-177.
- WEIKERT H. and TRINKHAUS S. 1990, Vertical mesozooplankton abundance and distribution in the deep Eastern Mediterranean Sea SE of Crete. Journal of Plankton Research 12, 601-628.
- WHEELER E.H. 1967, Copepod detritus in the deep sea. Limnology and Oceanography 12, 697-701.

- WIBORG K.F. 1951, The whirling vessel, an apparatus for the fractioning plankton samples. Fishkeridirektoratets Skrifter Serie Havundersokelser 9, 1-16.
- WIEBE P.H., MORTON A.W., BRADLEY A.M., BACKUS R.H., CRADOCK J.E., BARBER V., COWLES T.J. and FLIERL G.R. 1985, New developments in the MOCNESS, an apparatus for sampling zooplankton and micronekton. Marine Biology 87, 313-323.
- WROBLEWSKI J.S. 1980, A simulation of the distribution of *Acartia clausi* during Oregon upwelling in August 1973. Journal of Plankton Research 2, 43-68.
- WROBLEWSKI J.S. 1982, Interaction of currents and vertical migration in maintaining, *Calanus marshallae* in the Oregon upwelling zone - a simulation. Deep-Sea Research 29, 665-686.
- ZHAOLI X. and CHUNJU L. 2006, Study on the dominant species of Pteropoda in East China. Sea Chinese Journal of Oceanology and Limnology 24 (2), 168-177.

Acknowledgements - Danksagungen

Ich möchte mich bei Herrn Prof. Dr. von Elert bedanken, der mir durch die Betreuung, den großen Wunsch einer externen Bachelorarbeit in Hamburg ermöglicht hat. Danke auch an Herrn Prof. Dr. Arndt für das Zweitgutachten.

Weiterhin danke ich Herrn Prof. Dr. Christian Möllmann und Dr. Rolf Koppelman für das Anvertrauen des Themas und die Betreuung meiner Bachelorarbeit. Dabei möchte ich Rolf ganz herzlich für jedes Briefing danken.

Besonderer Dank geht an Herrn Prof. Dr. Herbert Fitzek, weil er mir als Papa, sowohl menschlich als auch fachlich, auf dem ganzen Weg zur Seite stand. Das ist unersetzlich.

Außerdem haben Dr. Bettina Martin und Silke Janßen dafür gesorgt, dass ich mich in der Arbeitsgruppe sehr wohl gefühlt habe.

Annethea Müller, vom Leibniz-Institut in Warnemünde, danke ich für die Bereitstellung der ozeanographischen Daten.

Danke auch an Freddi.

Appendix

Table A.1: Biomass of zooplankton in the MOCNESS nets in all sieve fractions expressed as wet weight (mg * 1000 m⁻³).

Net #	Fraction (mm)				
	< 0.5	0.5 - 1	1 - 2	2 - 5	Sum ≤ 5
L2	411.42	1731.32	1867.34	2703.61	6713.69
L4	1084.46	4414.34	5504.38	16670.92	27674.10
L5	889.16	3820.95	5758.83	10243.61	20712.55
L7	2218.22	2911.86	9434.32	20177.97	34742.37
L8	1758.20	3395.51	13156.21	24159.42	42469.33
R2	1232.34	4198.88	6269.52	19825.28	31526.02
R3	519.57	3040.36	13799.17	42283.51	59642.61
R4	1355.46	6735.25	33762.84	20229.78	62083.33
R5	1266.93	5561.03	17232.89	27229.99	51290.84
R6	3928.06	11082.01	23079.14	32805.76	70894.96
R8	2434.13	7688.62	11470.06	65149.70	86742.51

Table A.2: Abundances of zooplankton in the MOCNESS nets in all sieve fractions expressed as individuals * 1000 m⁻³.

Net #	Abundance (ind. * 1000 m ⁻³)					
	Fraction (mm)	< 0.5	0.5 - 1	1 - 2	2 - 5	Sum ≤ 5
L4		334.7	4908.4	3984.1	3872.5	13099.6
L5		667.5	8014.6	5127.9	3233.9	17043.9
L7		796.6	5788.2	9675.2	7457.6	23717.5
L8		2942.2	8880.2	20916.5	12582.0	45321.0
R4		1229.5	14672.1	68224.0	8242.3	92367.9
R6		25985.6	40863.3	25208.6	8906.5	100964.0
R8		14281.4	33682.6	15748.5	52874.3	116586.8

Table A.3: Total abundances of mesozooplankton in net L4 of the MOCNESS haul on October 3rd 2010 in all sieve fractions, expressed as individuals * 1000 m⁻³.

Taxon	Abundance (ind. * 1000 m ⁻³)				
	Fraction (mm)	< 0.5	0.5 - 1	1 - 2	2 - 5
Siphonophora (in parts)		0.0	0.0	0.0	15.9
Cnidaria		0.0	0.0	0.0	0.0
Ctenophora		0.0	0.0	0.0	0.0
Gelatinous undefined		0.0	0.0	0.0	0.0
Salpae		0.0	0.0	0.0	0.0
Appendicularia		0.0	0.0	0.0	0.0
Fish larvae		0.0	0.0	0.0	0.0
Fisheggs		0.0	31.9	0.0	0.0
Cephalopoda		0.0	0.0	0.0	0.0
Bivalvia		0.0	0.0	15.9	0.0
Other Mollusca		167.3	15.9	0.0	31.9
Chaetognatha		4.0	0.0	79.7	111.6
Polychaeta		0.0	15.9	0.0	15.9
Ostracoda		0.0	63.7	47.8	31.9
Isopoda		0.0	0.0	0.0	0.0
Amphipoda		0.0	31.9	207.2	175.3
Cladocera		0.0	0.0	0.0	0.0
Copepoda Calanoida		67.7	3840.6	2741.0	2565.7
Copepoda Cyclopoida		47.8	63.7	0.0	0.0
Copepoda Harpacticoida		0.0	0.0	0.0	0.0
Malacostraca &		47.8	844.6	605.6	510.0
Crustacea larvae					
Euphausiacea		0.0	0.0	286.9	414.3
Other larvae		0.0	0.0	0.0	0.0
Exuviae / carcasses		318.7	6661.4	2932.3	2884.5
Undefined		0.0	0.0	0.0	15.9

Table A.4: Total abundances of mesozooplankton in net L5 of the MOCNESS haul on October 3rd 2010 in all sieve fractions, expressed as individuals * 1000 m⁻³.

Taxon	Abundance (ind. * 1000 m ⁻³)				
	Fraction (mm)	< 0.5	0.5 - 1	1 - 2	2 - 5
Siphonophora (in parts)		0.0	0.0	0.0	42.6
Cnidaria		0.0	0.0	0.0	0.0
Ctenophora		0.0	0.0	0.0	6.1
Gelatinious undefinied		0.0	0.0	0.0	0.0
Salpae		0.0	0.0	0.0	0.0
Appendicularia		0.0	0.0	0.0	0.0
Fish larvae		0.0	0.0	12.2	0.0
Fisheggs		0.0	0.0	0.0	0.0
Cephalopoda		0.0	0.0	0.0	0.0
Bivalvia		0.0	0.0	0.0	0.0
Other Mollusca		170.5	73.1	48.7	18.3
Chaetognatha		19.5	97.4	97.4	237.5
Polychaeta		4.9	328.9	85.3	30.5
Ostracoda		24.4	73.1	24.4	18.3
Isopoda		0.0	0.0	0.0	0.0
Amphipoda		4.9	60.9	170.5	91.4
Cladocera		0.0	0.0	0.0	0.0
Copepoda Calanoida		209.5	5456.8	4007.3	1912.3
Copepoda Cyclopoida		87.7	60.9	0.0	6.1
Copepoda Harpacticoida		0.0	0.0	0.0	0.0
Malacostraca & Crustacea larvae		146.2	1814.9	548.1	219.2
Euphausiacea		0.0	24.4	109.6	682.1
Other larvae		0.0	0.0	0.0	0.0
Exuviae / carcasses		453.1	3520.1	1754.0	767.4
Undefined		0.0	24.4	24.4	12.2

Table A.5: Total abundances of mesozooplankton in net L7 of the MOCNESS haul on October 3rd 2010 in all sieve fractions, expressed as individuals * 1000 m⁻³.

Taxon	Abundance (ind. * 1000 m ⁻³)				
	Fraction (mm)	< 0.5	0.5 - 1	1 - 2	2 - 5
Siphonophora (in parts)		0.0	0.0	0.0	0.0
Cnidaria		0.0	0.0	0.0	0.0
Ctenophora		0.0	0.0	0.0	0.0
Gelatinous undefined		0.0	0.0	0.0	0.0
Salpae		0.0	0.0	0.0	0.0
Appendicularia		0.0	0.0	0.0	0.0
Fish larvae		0.0	0.0	0.0	0.0
Fisheggs		0.0	0.0	0.0	0.0
Cephalopoda		0.0	0.0	0.0	0.0
Bivalvia		0.0	0.0	0.0	0.0
Other Mollusca		33.9	118.6	127.1	42.4
Chaetognatha		59.3	254.2	466.1	423.7
Polychaeta		12.7	110.2	169.5	84.7
Ostracoda		8.5	42.4	113.0	42.4
Isopoda		0.0	0.0	0.0	0.0
Amphipoda		4.2	33.9	437.9	296.6
Cladocera		0.0	0.0	0.0	0.0
Copepoda Calanoida		334.7	4915.3	7401.1	4915.3
Copepoda Cyclopoida		334.7	237.3	98.9	0.0
Copepoda Harpacticoida		0.0	0.0	0.0	0.0
Malacostraca &		8.5	59.3	169.5	381.4
Crustacea larvae					
Euphausiacea		0.0	16.9	692.1	1228.8
Other larvae		0.0	0.0	0.0	0.0
Exuviae / carcasses		779.7	1932.2	1892.7	2669.5
Undefined		0.0	0.0	0.0	42.4

Table A.6: Total abundances of mesozooplankton in net L8 of the MOCNESS haul on October 3rd 2010 in all sieve fractions, expressed as individuals * 1000 m⁻³.

Taxon	Abundance (ind. * 1000 m ⁻³)				
	Fraction (mm)	< 0.5	0.5 - 1	1 - 2	2 - 5
Siphonophora (in parts)		0.0	0.0	17.8	28.5
Cnidaria		0.0	0.0	0.0	0.0
Ctenophora		0.0	0.0	0.0	0.0
Gelatinious undefinied		0.0	0.0	71.3	49.9
Salpae		0.0	0.0	0.0	0.0
Appendicularia		0.0	0.0	0.0	0.0
Fish larvae		0.0	0.0	17.8	35.7
Fisheggs		0.0	0.0	0.0	7.1
Cephalopoda		0.0	0.0	0.0	0.0
Bivalvia		0.0	0.0	0.0	0.0
Other Mollusca		89.2	107.0	214.0	57.1
Chaetognatha		0.0	71.3	445.8	798.9
Polychaeta		17.8	71.3	267.5	121.3
Ostracoda		17.8	214.0	338.8	42.8
Isopoda		0.0	0.0	0.0	0.0
Amphipoda		0.0	71.3	231.8	192.6
Cladocera		0.0	0.0	0.0	0.0
Copepoda Calanoida		873.8	6383.7	15674.0	7453.6
Copepoda Cyclopoida		1854.5	1587.0	3013.6	520.7
Copepoda Harpacticoida		0.0	0.0	0.0	0.0
Malacostraca & Crustacea larvae		89.2	356.6	374.5	199.7
Euphausiacea		0.0	0.0	249.6	3102.7
Other larvae		0.0	0.0	0.0	0.0
Exuviae / carcasses		303.1	1872.3	2692.6	1248.2
Undefined		0.0	17.8	17.8	0.0

Table A.7: Total abundances of mesozooplankton in net R4 of the MOCNESS haul on October 3rd 2010 in all sieve fractions, expressed as individuals * 1000 m⁻³.

Taxon Fraction (mm)	Abundance (ind. * 1000 m ⁻³)			
	< 0.5	0.5 - 1	1 - 2	2 - 5
Siphonophora (in parts)	0.0	0.0	54.6	54.6
Cnidaria	0.0	0.0	0.0	0.0
Ctenophora	0.0	0.0	0.0	0.0
Gelatinious undefined	0.0	0.0	0.0	0.0
Salpae	0.0	0.0	0.0	0.0
Appendicularia	0.0	0.0	0.0	0.0
Fish larvae	0.0	0.0	0.0	36.4
Fisheggs	0.0	0.0	0.0	0.0
Cephalopoda	0.0	0.0	0.0	0.0
Bivalvia	0.0	0.0	0.0	0.0
Other Mollusca	109.3	41.0	245.9	45.5
Chaetognatha	0.0	13.7	437.2	692.2
Polychaeta	0.0	95.6	273.2	36.4
Ostracoda	54.6	368.9	327.9	54.6
Isopoda	0.0	0.0	0.0	0.0
Amphipoda	0.0	82.0	382.5	300.5
Cladocera	0.0	0.0	0.0	0.0
Copepoda Calanoida	573.8	13265.0	63688.5	5264.1
Copepoda Cyclopoida	382.5	300.5	382.5	0.0
Copepoda Harpacticoida	0.0	0.0	0.0	0.0
Malacostraca & Crustacea larvae	109.3	505.5	1694.0	191.3
Euphausiacea	0.0	0.0	792.3	1621.1
Other larvae	0.0	0.0	0.0	0.0
Exuviae / carcasses	286.9	2636.6	6448.1	519.1
Undefined	0.0	0.0	0.0	0.0

Table A.8: Total abundances of mesozooplankton in net R6 of the MOCNESS haul on October 3rd 2010 in all sieve fractions, expressed as individuals * 1000 m⁻³.

Taxon	Abundance (ind. * 1000 m ⁻³)				
	Fraction (mm)	< 0.5	0.5 - 1	1 - 2	2 - 5
Siphonophora (in parts)		0.0	28.8	374.1	906.5
Cnidaria		0.0	0.0	0.0	0.0
Ctenophora		0.0	0.0	0.0	0.0
Gelatinous undefined		0.0	0.0	0.0	0.0
Salpae		0.0	0.0	0.0	0.0
Appendicularia		0.0	0.0	0.0	0.0
Fish larvae		0.0	0.0	0.0	86.3
Fisheggs		0.0	0.0	0.0	0.0
Cephalopoda		0.0	0.0	0.0	0.0
Bivalvia		0.0	0.0	0.0	0.0
Other Mollusca		3251.8	777.0	489.2	86.3
Chaetognatha		86.3	143.9	518.0	676.3
Polychaeta		115.1	259.0	287.8	71.9
Ostracoda		431.7	3050.4	518.0	43.2
Isopoda		0.0	0.0	0.0	0.0
Amphipoda		28.8	172.7	489.2	201.4
Cladocera		0.0	0.0	0.0	0.0
Copepoda Calanoida		17784.2	19741.0	19971.2	5295.0
Copepoda Cyclopoida		3453.2	8345.3	661.9	100.7
Copepoda Harpacticoida		0.0	0.0	0.0	0.0
Malacostraca & Crustacea larvae		805.8	8374.1	1352.5	143.9
Euphausiacea		0.0	0.0	920.9	2172.7
Other larvae		0.0	0.0	0.0	0.0
Exuviae / carcasses		1295.0	2014.4	1295.0	460.4
Undefined		28.8	0.0	0.0	28.8

Table A.9: Total abundances of mesozooplankton in net R8 of the MOCNESS haul on October 3rd 2010 in all sieve fractions, expressed as individuals * 1000 m⁻³.

Taxon	Abundance (ind. * 1000 m ⁻³)				
	Fraction (mm)	< 0.5	0.5 - 1	1 - 2	2 - 5
Siphonophora (in parts)		0.0	0.0	29.9	2694.6
Cnidaria		0.0	0.0	0.0	0.0
Ctenophora		0.0	0.0	0.0	0.0
Gelatinious undefined		0.0	0.0	0.0	0.0
Salpae		0.0	0.0	0.0	0.0
Appendicularia		0.0	0.0	0.0	0.0
Fish larvae		0.0	0.0	59.9	299.4
Fisheggs		0.0	0.0	0.0	0.0
Cephalopoda		0.0	0.0	0.0	0.0
Bivalvia		0.0	0.0	0.0	0.0
Other Mollusca		1886.2	1227.5	0.0	1976.0
Chaetognatha		119.8	299.4	149.7	1916.2
Polychaeta		0.0	239.5	149.7	658.7
Ostracoda		239.5	1856.3	59.9	1916.2
Isopoda		0.0	0.0	0.0	0.0
Amphipoda		0.0	209.6	209.6	479.0
Cladocera		0.0	0.0	0.0	0.0
Copepoda Calanoida		1646.7	20329.3	13383.2	32095.8
Copepoda Cyclopoida		10059.9	7994.0	928.1	8383.2
Copepoda Harpacticoida		0.0	0.0	0.0	0.0
Malacostraca &		329.3	1467.1	449.1	1676.6
Crustacea larvae					
Euphausiacea		0.0	29.9	359.3	3293.4
Other larvae		0.0	0.0	0.0	0.0
Exuviae / carcasses		838.3	1646.7	389.2	4850.3
Undefined		0.0	29.9	0.0	179.6

Table A.10: Abundances of Chaetognatha expressed as individuals * 1000 m⁻³. in sieve fractions in averages and sum of fractions <5 mm in water mass 'A' (WMA: L4, L5, L7) and water mass 'B' (WMB: R4, R6, R8). P-values for the single fractions were adjusted according to *Bonferroni*.

Abundance (ind. *1000 m⁻³)			
Fraction (mm)	WMA	WMB	t-test
			WMA vs. WMB
< 0.5	27.6	68.7	1.000
0.5 - 1	117.2	152.3	1.000
1 - 2	214.4	368.3	1.000
2 - 5	257.6	684.2	0.193
Sum < 5	616.8	1684.2	0.133

Table A.11: Abundances of Euphausiacea expressed as individuals * 1000 m⁻³. in sieve fractions in averages and sum of fractions <5 mm in water mass 'A' (WMA: L4, L5, L7) and water mass 'B' (WMB: R4, R6, R8). P-values for the single fractions were adjusted according to *Bonferroni*.

Abundance (ind. *1000 m⁻³)			
Fraction (mm)	WMA	WMB	t-test
			WMA vs. WMB
< 0.5	0.0	0.0	<i>N/A</i>
0.5 - 1	13.8	10.0	1.000
1 - 2	362.9	690.8	1.000
2 - 5	775.1	1896.9	0.174
Sum < 5	1151.7	3063.2	0.063

Eidesstattliche Erklärung

Ich erkläre hiermit, dass ich diese Bachelorarbeit selbstständig, ohne Hilfe Dritter und ohne Benutzung anderer als den angegebenen Quellen und Hilfsmitteln verfasst habe. Alle benutzten Quellen, wörtlich oder sinngemäß entnommene Stellen, sind als solche einzeln kenntlich gemacht.

Diese Arbeit ist bislang keiner anderen Prüfungsbehörde vorgelegt worden und auch nicht veröffentlicht worden.

Ich bin mir bewusst, dass eine falsche Erklärung rechtliche Folgen haben wird.

Hamburg, den 26. Mai 2011

(Sarah Fitzek)